EXPLANATORY NOTES

GOVERNMENT OF WESTERN AUSTRALIA

GEOLOGY OF THE JOHNSTON RANGE 1:100 000 SHEET

by S. Wyche, S. F. Chen, J. E. Greenfield, and A. Riganti

1:100 000 GEOLOGICAL SERIES

GEOLOGICAL SURVEY OF WESTERN AUSTRALIA

DEPARTMENT OF MINERALS AND ENERGY

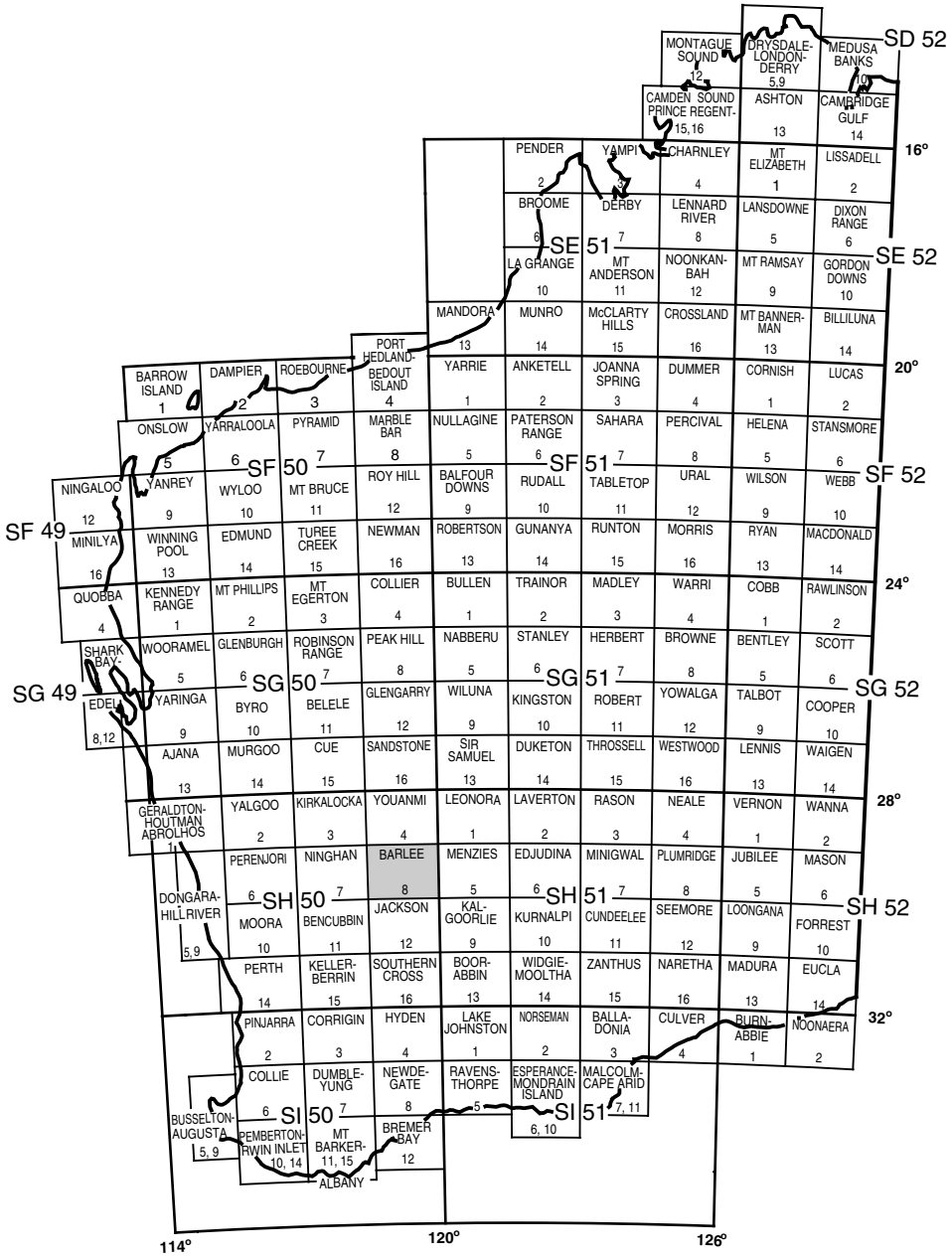

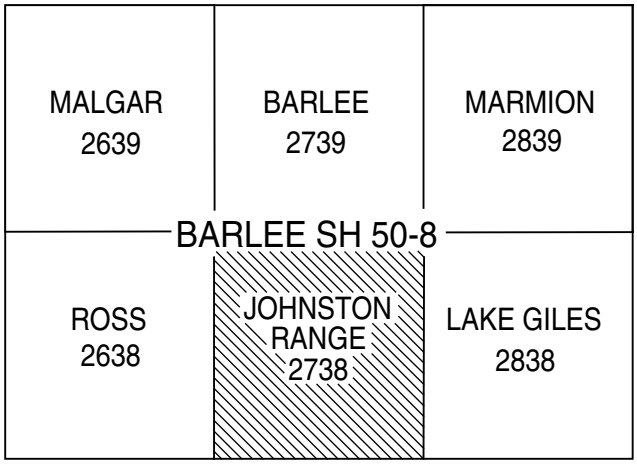

SW136

27.03.01

GEOLOGICAL SURVEY OF WESTERN AUSTRALIA

GEOLOGY OF THE JOHNSTON RANGE 1:100 000 SHEET

by
S. Wyche, S. F. Chen, J. E. Greenfield, and A. Riganti

Perth 2001

MINISTER FOR STATE DEVELOPMENT; TOURISM; SMALL BUSINESS; GOLDFIELDS–ESPERANCE
The Hon. Clive Brown MLA

DIRECTOR GENERAL
L. C. Ranford

DIRECTOR, GEOLOGICAL SURVEY OF WESTERN AUSTRALIA
Tim Griffin

Copy editor: C. D'Ercole

REFERENCE
The recommended reference for this publication is:
WYCHE, S., CHEN, S. F., GREENFIELD, J. E., and RIGANTI, A., 2001, Geology of the Johnston Range 1:100 000 sheet: Western Australia Geological Survey, 1:100 000 Geological Series Explanatory Notes, 31p.

National Library of Australia Card Number and ISBN 0 7307 5676 9

ISSN 1321–229X

Grid references in this publication refer to the Geocentric Datum of Australia 1994 (GDA94). Locations mentioned in the text are referenced using Map Grid of Australia (MGA) coordinates, Zone 50. All locations are quoted to at least the nearest 100 m

Printed by Optima Press, Perth, Western Australia

Copies available from:
Information Centre
Department of Minerals and Energy
100 Plain Street
EAST PERTH, WESTERN AUSTRALIA 6004
Telephone: (08) 9222 3459 Facsimile: (08) 9222 3444
www.dme.wa.gov.au

Cover photograph:
Ridge of banded iron-formation in the Die Hardy Range (photo north from MGA 728300E 6690000N)

Contents

Appendices

Figures

Table

Geology of the Johnston Range 1:100 000 sheet

by

S. Wyche, S. F. Chen, J. E. Greenfield, and A. Riganti

Abstract

The JOHNSTON RANGE 1:100 000 sheet lies within the Southern Cross Province in the central part of the Archaean Yilgarn Craton. The sheet covers a poorly exposed granite–greenstone terrain in which an older, mafic-dominated greenstone succession and a younger, felsic volcanic- and clastic sedimentary-dominated greenstone succession are in faulted or intrusive contact with mainly younger granitoid rocks of dominantly monzogranitic composition.

The lower greenstone succession includes metamorphosed basalt, high-Mg basalt, ultramafic rock, sedimentary rock (including prominent ridges of banded iron-formation and chert), and minor felsic volcanic and intrusive rock. Although the age is poorly constrained, this succession is probably about 3.0 Ga. The upper greenstone succession includes metamorphosed felsic volcanic and volcaniclastic rocks of the calc-alkaline Marda Complex, and metamorphosed clastic sedimentary rocks of the Diemals Formation. All of these rocks were deposited at c. 2.73 Ga. An unconformity between the lower greenstone succession and Diemals Formation is preserved locally.

Greenstones on JOHNSTON RANGE record a multistage, regional deformation regime. In the first stage (D_1), north–south compression produced a layer-parallel foliation and tight to isoclinal folds. This was followed by an extended period of east–west compression that can be described in terms of two major deformation events: large-scale upright folding (D_2); and movement on the regional-scale faults and shear zones, and reorientation of earlier structures (D_3). These deformation events were largely responsible for the present-day granite–greenstone architecture. Subsequent deformation included the development of north-northeasterly and east-southeasterly trending faults and fractures during east–west to east-northeast – west-southwest compression (D_4), and other, less well-defined structures whose absolute age is uncertain. Mafic and ultramafic dykes of probable Proterozoic age occupy late, easterly to northeasterly trending fractures.

Some granitoid intrusion took place at the time of the deposition of the upper greenstone succession, but most of the granitoids appear to have intruded the succession after c. 2.7 Ga.

All greenstones have been metamorphosed, with grades ranging from very low (prehnite–pumpellyite facies) to high (amphibolite facies). However, the higher grade rocks contain high-temperature, low-pressure assemblages, indicating that none of the greenstones have been deeply buried.

Gold has been produced from a number of localities on JOHNSTON RANGE, but no large deposits have been discovered. Although several base metal occurrences have been found, no economic concentrations have been identified.

KEYWORDS: Archaean, granite, greenstone, Southern Cross Province, Marda, Diemals

Introduction

The JOHNSTON RANGE* 1:100 000 sheet (SH 50-8, 2738) occupies the central-southern part of the BARLEE 1:250 000 sheet between latitudes 29°30'S and 30°00'S, and longitudes 119°00'E and 119°30'E. The only permanent settlement on JOHNSTON RANGE is Diemals Homestead in the central-northern part of the sheet area (Fig. 1).

The first European to traverse the area was the explorer Ernest Giles in 1875 (Giles, 1889). The earliest published geological descriptions of the area are those of Talbot (1912), Woodward (1912), and Blatchford and Honman (1917). Matheson and Miles (1947) described gold mines

* Capitalized names in these notes refer to standard 1:100 000 map sheets, unless otherwise stated.

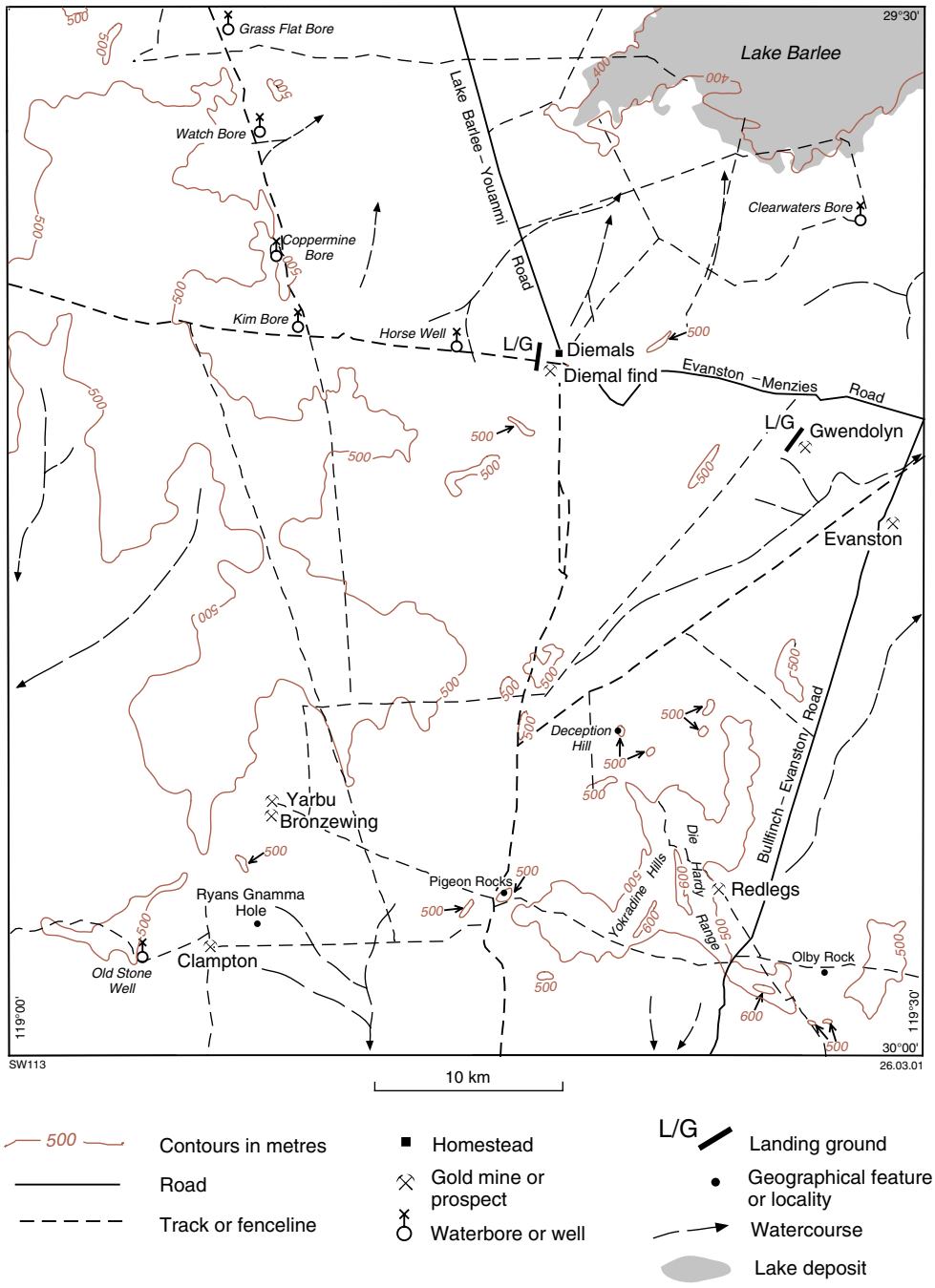

Figure 1. Principal localities, roads, and physiographic features on JOHNSTON RANGE

in the district, but the first published geological map was the first edition of the BARLEE 1:250 000 sheet (Walker and Blight, 1983). Ahmat (1986) investigated the regional distribution of metamorphic grade in a study that utilized the extensive Geological Survey of Western Australia's (GSWA) thin-section collection. A more-detailed study of metamorphic patterns between Southern Cross and Diemals (Dalstra, 1995; Dalstra et al., 1999) also examined the structural evolution of the area, and controls on gold mineralization.

Mineral exploration on JOHNSTON RANGE has been directed mainly towards the discovery of gold and base metal deposits. Unpublished maps and data produced as a result of mineral exploration are available through the Western Australian mineral exploration (WAMEX) open-file database at the Department of Minerals and Energy's library in Perth, and at the GSWA Kalgoorlie Regional Office.

Mapping of JOHNSTON RANGE was carried out between July and November 1997, with follow-up fieldwork in mid-1998 using 1:25 000-scale, colour aerial photographs commissioned by the Department of Land Administration (DOLA) in 1994–95, complemented by Landsat Thematic Mapper (TM5) images, and 400 m line-spaced aero-

magnetic data acquired by Kevron Geophysics Pty Ltd in 1997, which are available for purchase from the Australian Geological Survey Organisation (AGSO). Cuttings from mineral-exploration drillholes were examined where they have been preserved at the drill site. Selected examples have been shown on the map to elucidate subsurface geology in areas of poor outcrop.

Access to JOHNSTON RANGE is provided by formed roads from Menzies (160 km) to the east of the eastern edge of the sheet area, Bullfinch (125 km) and Southern Cross (158 km) to the south of the southern edge of the sheet area, and Youanmi and Sandstone to the north. Access to areas underlain by greenstones is commonly available along station and mineral-exploration tracks. Some areas, particularly those with abundant banded iron-formation (BIF) and chert, are covered by dense scrub that can be difficult to penetrate. Access to areas underlain by granitoid rocks is restricted to a few station tracks.

Climate, physiography, and vegetation

The region that includes JOHNSTON RANGE has a semi-arid climate*. Diemals Homestead has an average annual rainfall of 276 mm, with the wettest months between April and August. However, major summer rainfall events due to tropical influences from the north are not uncommon. The hottest months are from December to March when temperatures regularly exceed 40°C, and the coldest months from June to August when there are occasional frosts.

Relief over most of the sheet area is low, but there are substantial ridges and ranges in the southeast, the Die Hardy Range and Yokradine Hills (Fig. 1), where elevations range up to about 640 m above the Australian Height Datum (AHD). The lowest points (~400 m) lie in Lake Barlee in the northeast. Drainage in the north is to the northeast towards Lake Barlee, which is part of the Raeside Palaeoriver system (Hocking and Cockbain, 1990), whereas drainage in the south is mainly to the south. Away from areas of greenstone, sand- and loam-covered plateaus with breakaways are underlain by lateritic duricrust developed over granitoid rock.

The northern part of JOHNSTON RANGE lies within the Austin Botanical District, or Murchison Region, of the Eremaean Province of Beard (1990). This region is characterized by extensive woodlands dominated by mulga (*Acacia aneura*), with sparse, low shrub that may include *Acacia*, *Cassia*, and *Eucalyptus* species, along with ephemeral herbs and sparse perennial and annual grasses. Spinifex grass may grow in areas of extensive sandplain. Mulga scrub is abundant in areas underlain by granitoid rocks, but a greater variety of vegetation is found over the greenstone belts. *Eucalyptus* replace mulga as the dominant tree type in the southern part of JOHNSTON RANGE, which lies in the Coolgardie Botanical District, or Southwestern Interzone, of Beard (1990).

* Climate data from Commonwealth Bureau of Meteorology website, 2000.

Precambrian geology

Regional geological setting

JOHNSTON RANGE lies within the Southern Cross Province of Gee et al. (1981) in the central part of the Yilgarn Craton, and includes most of the Diemals greenstone belt and part of the Marda greenstone belt of Griffin (1990). The Southern Cross Province is separated from the Eastern Goldfields Province to the east on the basis of differences in the range of rock types, the relative volumes of different rock types, age of the greenstone sequences, and structural style. The boundary between the provinces is taken to be the Ida Fault, a regional-scale feature that lies about 100 km to the east of JOHNSTON RANGE (Fig. 2; Wyche, 1999).

There is no published stratigraphy for the central Yilgarn, but it has long been recognized that there are two supracrustal sequences in the Marda–Diemals region (Fig. 2), separated by a major unconformity (Hallberg et al., 1976; Chin and Smith, 1983; Walker and Blight, 1983; Griffin, 1990). The lower greenstone succession contains mafic and ultramafic rocks, clastic sedimentary rocks, chert, BIF, and minor felsic volcaniclastic rocks. The upper greenstone succession includes the felsic volcanic and associated volcaniclastic rocks of the Marda Complex (Hallberg et al., 1976), and the clastic sedimentary rocks of the Diemals Formation (Walker and Blight, 1983).

The limited amount of published sensitive high-resolution ion microprobe (SHRIMP) U–Pb zircon geochronology suggests that the lower greenstone sequence was deposited c. 3.0 Ga (Wang et al., 1996; Nelson, 1999), while the conventional U–Pb zircon age of 2735 ± 2 Ma for the Marda Complex (Pidgeon and Wilde, 1990) is supported by more recent SHRIMP data that gives an age of c. 2733 Ma (Nelson, in prep.).

Recent studies of the structural evolution of the Marda–Diemals area have identified a multistage, regional deformation history (Dalstra, 1995; Dalstra et al., 1999; Greenfield and Chen, 1999; Chen et al., 2001; Table 1). In the first stage (D_1), north–south compression produced tight to isoclinal folds, and may have initiated development of some of the large-scale shear zones that are prevalent throughout the central Yilgarn Craton. Following this, an extended period of east–west compression produced large-scale upright folding (D_2), and regional-scale faults and shear zones, and reorientation of earlier structures (D_3). Deposition of the upper greenstone succession probably commenced during early D_2. Subsequent deformation included the development of north-northeasterly and east-southeasterly trending faults and fractures during east–west to east-northeast – west-southwest compression (D_4), and the development of a locally recognized, late-stage, easterly trending foliation with associated crenulation and open folding. However, the order and absolute timing of these latter events is unclear. Dykes of probable Proterozoic mafic and ultramafic rocks occupy easterly to

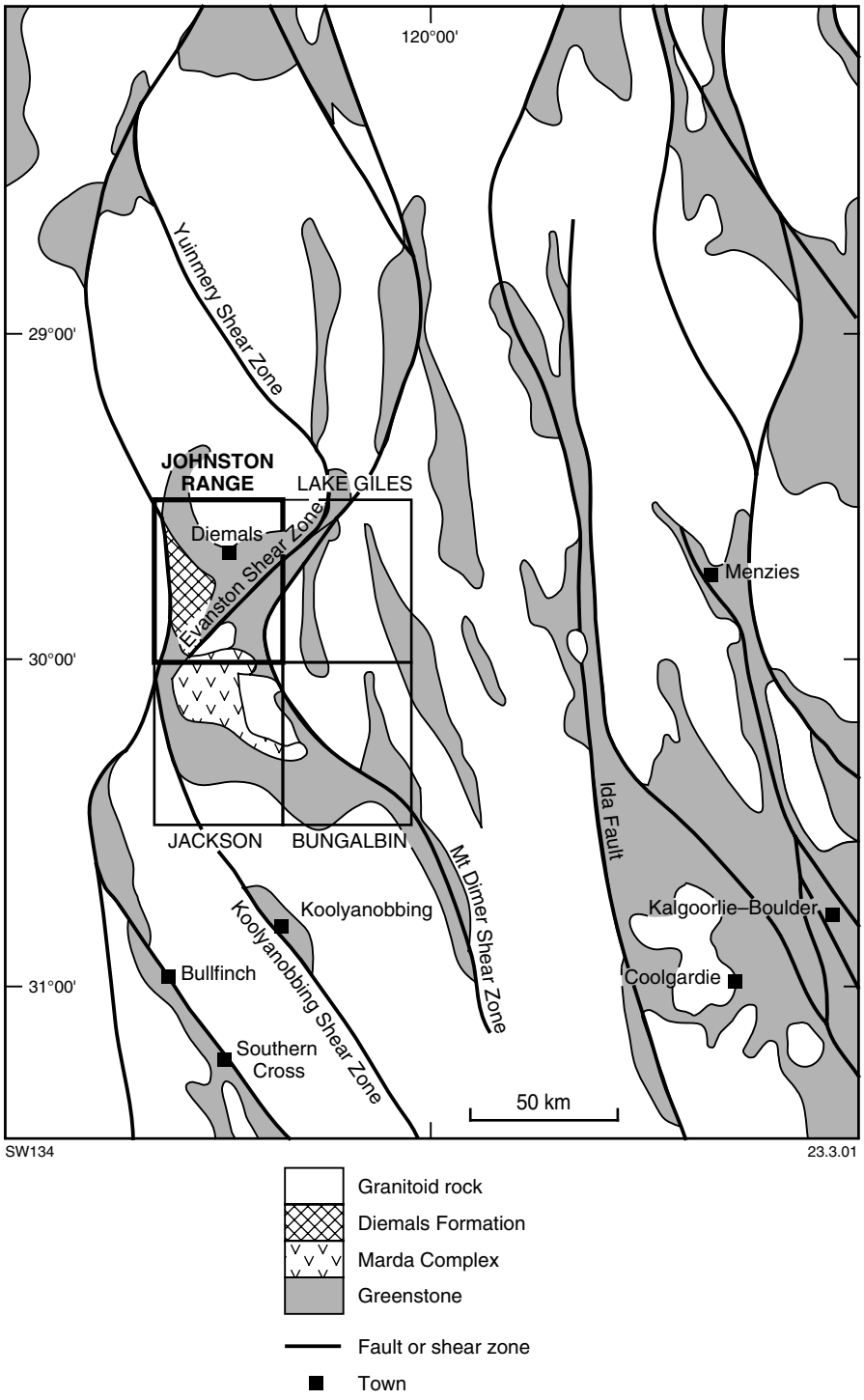

Figure 2. Regional setting of JOHNSTON RANGE

northeasterly trending fractures that overprint all earlier structures.

Archaean rock types

All Archaean rocks described in these Explanatory Notes have been subjected to low- to medium-grade metamorphism. However, for ease of description, the prefix 'meta-' may be omitted.

Lower greenstone succession

Metamorphosed ultramafic rocks (Au, Aup, Aur, Aus, Aut)

Metamorphosed ultramafic rocks, although not as abundant as mafic volcanic and intrusive rocks, are widespread in the lower greenstone sequence, and are particularly abundant (commonly in association with high-Mg basalt) adjacent to units of BIF.

Table 1. Geological evolution of Johnston Range

Age	*Deformation event*	*Geology*
c. 3.0 Ga		Deposition of the lower greenstone succession; burial/seafloor metamorphism
	D_1	Layer-parallel foliation and thrusting; tight to isoclinal folding
	D_2	Initiation of east–west compressional regime Upright to inclined folding
c. 2.73 Ga		Granitoid intrusion Deposition of upper greenstone succession; Marda Complex (felsic volcanism) and Diemals Formation (clastic sedimentary rocks)
c. 2.71 Ga – c. 2.65 Ga		Granitoid intrusion; peak metamorphism
Pre- c. 2656 Ma	D_3	Development of major northeasterly and northwesterly trending shear zones; reorientation of D_2 structures
	D_4	North-northeasterly and east to east-southeasterly trending brittle faults Intrusion of easterly to northeasterly trending mafic and ultramafic dykes along cross-cutting fractures

Where metamorphosed ultramafic rocks are shown as undivided (*Au*) on the map, they are typically deeply weathered and identified on the basis of their association with less-weathered ultramafic rocks, and their chlorite content. Where their mineralogy is better preserved, ultramafic rocks are classified according to the most distinctive mineral species present (e.g. chlorite, talc, tremolite), except in the case of peridotite (*Aup*), which preserves relict cumulate textures despite pervasive serpentinization. Peridotite also contains interstitial clinopyroxene (2–5%) and chlorite (<1%) between the olivine pseudomorphs, as well as secondary magnetite (2–5%).

Tremolite–chlorite(–talc) schist (*Aur*) outcrops locally, but the freshest examples are typically found in cuttings from mineral-exploration drillholes. Where fresh, fine- to coarse-grained tremolite forms aggregates and fans of elongate crystals that define the foliation, with abundant interstitial chlorite and opaque oxides (typically magnetite) that may constitute up to 10% of the rock. Talc or plagioclase may be minor constituents. These rocks are probably derived from ultramafic volcanic rocks, but examples with feldspar may be the result of metamorphism and deformation of high-Mg basalt. Serpentinite (*Aus*) consists of massive, microcrystalline, matted aggregates of serpentine that may contain scattered, fine-grained opaque oxides and minor biotite. No primary igneous textures are preserved. Talc–tremolite (–chlorite) schist (*Aut*) is typically a strongly deformed ultramafic rock with talc as a prominent mineral species.

Metamorphosed, fine-grained mafic rocks (Ab, Aba, Abar, Abe, Abf, Abi, Abm, Abmf, Abr, Abrc, Abt, Abv, Abx)

Metamorphosed, fine-grained mafic rocks are widely distributed in the lower greenstone sequence on Johnston Range, and are found at all stratigraphic levels.

Undivided mafic rocks (*Ab*) are typically too weathered to allow primary mineralogy and textural features to be distinguished. They are described as mafic because they lack primary quartz, and may contain chlorite. Some may be sedimentary rocks with a mafic provenance.

Metabasalt (*Abv*) is typically fine to medium grained, and consists of pale- to dark-green amphibole, and plagioclase, which may form fine laths or be interstitial to the amphibole. Metabasalt typically contains minor (up to about 5%) opaque oxides. Relict intergranular to subophitic textures can be seen commonly in thin sections, but larger-scale igneous textures are rarely well preserved (e.g. possible relict amygdales are filled by chlorite, sericite, and epidote at MGA 730400E 6698000N). Chlorite is a common product of retrograde metamorphism.

South of Diemals Homestead (e.g. around MGA 722800E 6714500N), several thin units of metamorphosed mafic tuff (*Abt*) are found within a sequence of basalt flows of probable tholeiitic composition. The tuffaceous rocks are pale grey, very fine grained, and thin bedded and laminated (5 cm to >1 mm scale bedding). Some outcrops contain small angular clasts (<5 mm across) of similar material, and cross-beds are preserved locally. Rounded voids up to 5 mm across, locally filled with clay and locally cut across bedding features, may represent either devitrification effects or the result of later alteration. Chemical analyses of these rocks (see GSWA 143376 and 143377 in Appendix 2) indicate compositions in the basaltic andesite range, but the silica content may have been modified by post-depositional alteration.

Fine-grained, metamorphosed basaltic andesite (*Abi*) is distinguished from metabasalt by its paler colour (light to medium grey) and plagioclase microlithic texture. Plagioclase is the dominant phase (up to 50%), typically

as aligned, slender laths. Tremolite–actinolite constitutes up to 30% of the rock, with granoblastic quartz aggregates and accessory phases (opaque oxides, biotite, chlorite) making up the remainder. Small outcrops of basaltic andesite are found intercalated within mafic and ultramafic rocks to the northeast of the Clampton mine.

Metamorphosed high-Mg basalt (*Abm*) is characterized by the presence of relict pyroxene-spinifex texture, either randomly oriented or in sheaves, in which tremolite–actinolite has replaced acicular pyroxene grains. Spinifex-texture needles range from less than 1 mm to more than 1 cm long. Metamorphosed high-Mg basalt may also preserve variolitic texture consisting of leucocratic, spheroidal aggregates of microcrystalline feldspar and amphibole. The typical mineral assemblage includes tremolite–actinolite, chlorite, and subordinate plagioclase, which forms fine-grained aggregates between the mafic grains. Minor opaque oxides and epidote may also be present. High-Mg basalt typically contains between 10 and 18% MgO (equivalent to the komatiitic basalt of Arndt and Nisbet, 1982; Cas and Wright, 1987; see Appendix 2). Strongly deformed high-Mg basalt (*Abmf*) has been mapped only where clear relict pyroxene-spinifex, variolitic textures or both are preserved. Strongly deformed mafic rock that contains tremolite, chlorite, and plagioclase (*Abr*) may be derived from high-Mg basalt, but no relict igneous textures are preserved. These rocks may also contain biotite, epidote, titanite, talc, and opaque oxides. Tremolite–actinolite may be strongly aligned parallel to foliation, or randomly oriented in radiating aggregates of acicular crystals. This rock type is strongly carbonated (*Abrc*) in the area just south of the Redlegs prospect (around MGA 730500E 6687000N), where it contains coarsely crystalline carbonate minerals, mainly calcite and dolomite.

Amphibolite (*Aba*) is widespread in the Evanston district, mainly as dark-green, strongly foliated rocks in low outcrops. The mineralogy is dominated by ragged patches of blue-green actinolite and squat, light-brown to green pleochroic hornblende crystals, with minor plagioclase, magnetite, and quartz. Some actinolite needles have overprinted the main tectonic fabric suggesting post-kinematic metamorphism of these rocks.

Along the granite–greenstone contact near the Clampton mine, rocks of amphibolitic appearance, but distinguished by greenschist facies mineral assemblages (*Abar*), are typically dark grey, and commonly have a strong fabric defined by segregations of plagioclase and amphibole into layers up to a few millimetres thick. Frayed and deformed grains of tremolite–actinolite dominate, with actinolitic hornblende only locally preserved. Quartz and finer amphibole are interstitial; epidote minerals and chlorite are developed locally. These rocks have a basaltic chemistry (e.g. GSWA 153299 in Appendix 2).

Strongly epidotized metabasalt (*Abe*), 6 km west of Deception Hill (MGA 719500E 6698500N), outcrops on both sides of a BIF ridge as light-green, weathered, fine-grained mafic rock. Abundant, thin epidote veins (0.1 – 0.2 cm wide) intrude the metabasalt, along with minor quartz veins. In thin section, the epidotized metabasalt consists of acicular tremolite–actinolite, plagioclase, and minor opaque oxides, with disseminated, fine-grained, prismatic epidote grains.

Metamorphosed mafic rock that is strongly foliated (*Abf*) is typically found along strongly deformed granite–greenstone contacts. Such rocks may be fine to coarse grained, and consist of recrystallized plagioclase, amphibole (ranging from tremolite–actinolite to hornblende, depending on the protolith), and minor opaque oxides. Although metamorphic grade is dominantly in the greenschist facies, some of these rocks are strongly recrystallized with dark-bluish-green, strongly pleochroic hornblende, suggesting that they have been metamorphosed to the amphibolite facies. Strongly foliated mafic rock (*Abf*) may be intercalated with less-deformed metabasalt with relict igneous textures.

A single outcrop of mafic breccia (*Abx*) west of Gwendolyn Mine (MGA 730800E 6711500N) has been interpreted as a flow-top breccia by Walker and Blight (1983). The breccia contains centimetre-scale, subrounded clasts with a uniform, fine- to medium-grained texture of decussate actinolite needles. The matrix contains medium-grained anthophyllite, zoisite, plagioclase, and radiating clusters of colourless tremolite needles. Zoisite has a deep-blue interference colour and consists of euhedral, squat prisms. A narrow (<1 cm wide) alteration halo containing zoisite and actinolite surrounds the matrix assemblage, suggesting metamorphic fluids may have been focused into the matrix during metasomatism. The rock has been deformed, resulting in a broad alignment of the clasts, although the foliation is not pervasive. Late, narrow (1–3 mm wide) quartz veins crosscut the breccia. The veins are discontinuous and evenly spaced on a centimetre scale.

Metamorphosed, medium- to coarse-grained mafic rocks (Ao, Aog)

Metamorphosed, medium- to coarse-grained mafic rocks on Johnston Range are confined to the lower greenstone succession, where they form both discrete sill-like units and coarser intervals and lenses within finer-grained mafic rocks. The sill-like bodies are particularly common at the same stratigraphic level as the major units of BIF (e.g. in the Die Hardy Range and Watch Bore Syncline; Figs 3 and 4) where they appear to have intruded into and along bedding planes.

In the Die Hardy Range, a 1 m-thick unit of BIF rests within metagabbro between the two major BIF intervals. The thin BIF unit is locally disrupted, but can be traced over a strike length of up to 10 km. However, it is not clear whether the gabbro above and below the BIF represents one or more intrusive episodes. Similar occurrences of BIF within gabbro are common in the relatively well-exposed eastern limb of the Watch Bore Syncline.

Deeply weathered metagabbro (*Ao*) is most commonly found adjacent to ridges of BIF. Most of the original mineralogy has been altered in these rocks, but, although commonly deformed, the lack of primary quartz and relict medium- to coarse-grained texture suggest that they represent gabbroic or pyroxenitic rocks.

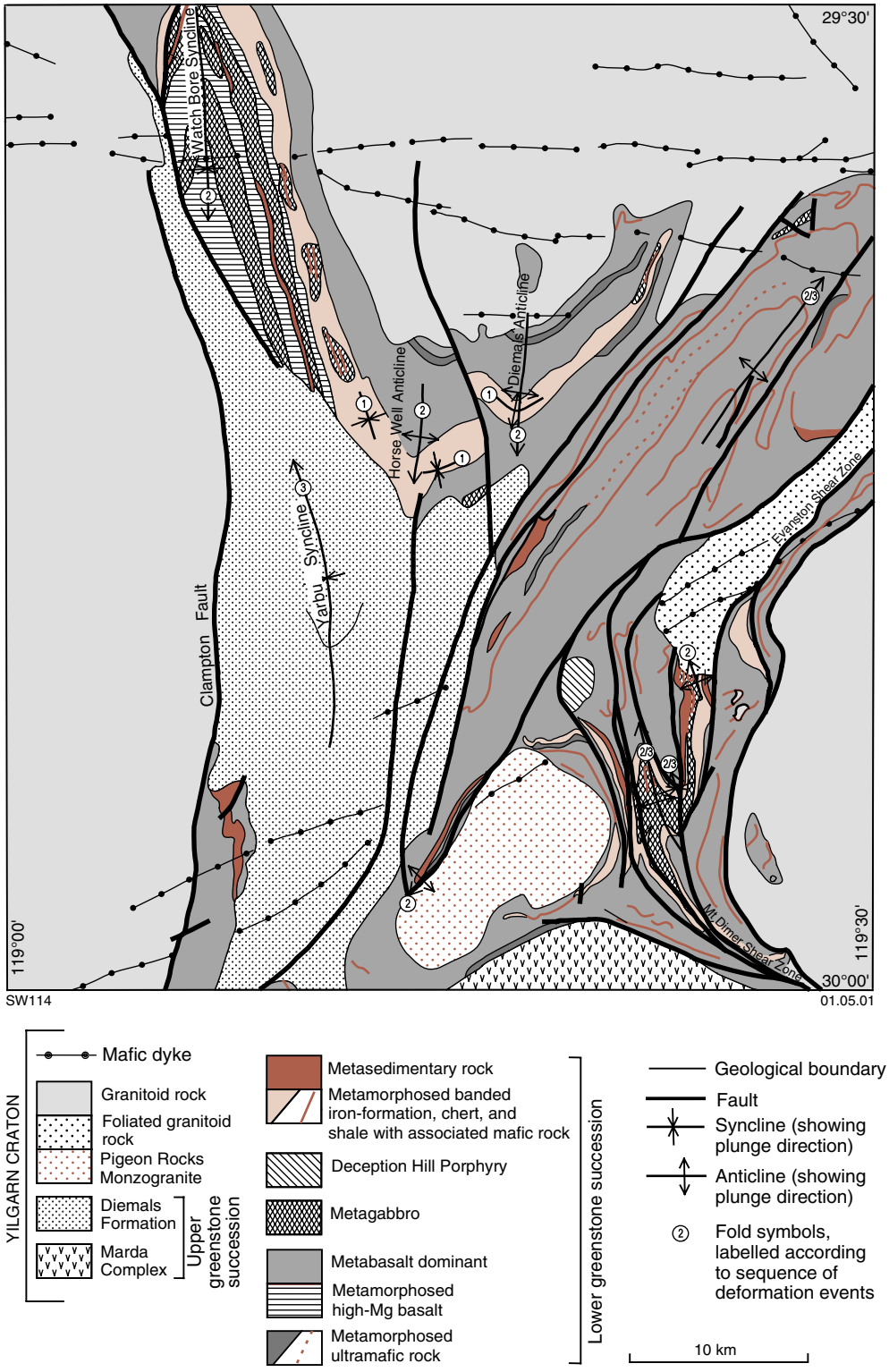

Figure 3. Simplified geological map of Johnston Range

Metagabbro (*Aog*) commonly preserves primary clinopyroxene in both the Die Hardy Range and Watch Bore areas. Distinctive melanocratic metagabbro forms a marker horizon in the Die Hardy Range, where it may represent part of a differentiated sill as it is associated with local outcrops of more leucocratic, locally quartz-bearing gabbro with a euhedral granular texture (e.g. in the fold hinge at the northern end of the Die Hardy Range at MGA 728900E 6691500N). However, the outcrop is poor and discontinuous, and so it is difficult to identify a clear differentiation trend. The typical metagabbro in this area is fine to medium grained with local coarse-grained

Figure 4. Grey-scale aeromagnetic map of total magnetic intensity for JOHNSTON RANGE

intervals. Clinopyroxene, which may comprise more than 80% of the rock, is commonly altered to chlorite and tremolite. However, where relict grains are preserved, it is pale brown to pale green, and probably augitic in composition. In the most abundant variety of gabbro, finer grained plagioclase is interstitial to the clinopyroxene, and some samples contain abundant (up to 15%) opaque oxides including magnetite (partly altered to goethite) and ilmenite (partly altered to leucoxene). Apart from tremolite and chlorite, epidote is a common secondary mineral. The melanocratic metagabbro is a distinctive rock type with a characteristic cumulate texture, with feldspar occupying interstices between the mafic minerals.

Medium- to coarse-grained metagabbros are well exposed in the northwestern part of JOHNSTON RANGE. In

the eastern limb of the Watch Bore Syncline, gabbro sills have intruded between chert and BIF horizons. There are two major layered gabbro sills, each of which is up to 1 km in thickness. The lower gabbro sill typically contains acicular clinopyroxene crystals up to 20 cm long in a medium- to coarse-grained matrix. Locally preserved igneous layering, defined by differentiation of leucocratic and melanocratic gabbro, is concordant with the underlying shale. The upper gabbro sill, in the core of the syncline, is concordant with both the underlying and overlying high-Mg basalts.

A metagabbro unit that overlies BIF and quartzite units west of the Pigeon Rocks Monzogranite is medium grained and equigranular. Pyroxene, now replaced by light- to mid-green amphibole, which makes up about 70% of the rock, preserves a relict subophitic texture. Ilmenite, commonly replaced by leucoxene, is an abundant accessory mineral.

In other areas, metagabbro is fine to medium grained, equigranular, with approximately equal proportions of plagioclase and ragged, light- to mid-green, pleochroic amphibole grains (after pyroxene), accessory opaque oxides, and local minor biotite. Mafic minerals have commonly undergone retrograde metamorphism to chlorite. A small, poorly outcropping patch of altered, plagioclase-phyric plagioclase–amphibole–quartz rock south of Deception Hill (at MGA 724300E 6692600N), mapped as metagabbro, may originally have been a quartz diorite.

Metamorphosed felsic rocks (Af, Afv, Apdh)

Metamorphosed felsic volcanic and intrusive rocks make up a relatively small proportion of the lower greenstone succession on JOHNSTON RANGE. They are typically weathered or altered, and original textures are difficult to recognize. Deeply weathered felsic rocks are classified as undivided (*Af*) where there are no clear igneous textures preserved, but quartz is a common constituent.

Metamorphosed, fine-grained felsic volcanic rocks (*Afv*) north and west of Ryans Gnamma Hole are typically pale grey to white and have locally preserved flow banding. They commonly contain rounded quartz phenocrysts up to 2–3 mm across (some with embayed outlines) in a fine, granoblastic, sericitic, and quartz-rich groundmass, suggesting a possible rhyolitic composition. Sericite also pseudomorphs millimetre-scale, prismatic feldspar grains, some of which preserve relict Carlsbad twinning. It is possible that some of these felsic units may have been tuffs or locally derived volcaniclastic rocks. The felsic volcanic horizons are typically only a few metres thick, and are characteristically intercalated within the shaly metasedimentary unit exposed to the northeast of Clampton mine. A notable exception is represented by a 14 m-thick, crystal tuff horizon and associated metasedimentary unit, flanked by mafic volcanic rocks, which are intermittently exposed approximately 1 km west of Ryans Gnamma Hole (MGA 705670E 6686710N). The crystal tuff consists of tightly packed idiomorphic feldspar (mainly sericitized plagioclase) and subordinate, rounded, locally corroded quartz phenocrysts up to 5 mm in size, set in a dark-grey quartz–sericite–feldspar groundmass; biotite is also present. The crystal tuff grades laterally into banded chert with fine tuffaceous intercalations, which in turn grades eastwards into fine- to medium-grained, quartz-rich sandstone.

The Deception Hill Porphyry (*Apdh*) forms a prominent, isolated hill in the southeastern quadrant of JOHNSTON RANGE (Fig. 1). The porphyry consists of phenocrysts of plagioclase (now albite) and quartz set in a fine-grained quartzofeldspathic matrix. Plagioclase phenocrysts are much more abundant than quartz phenocrysts. Scattered, fine mafic phenocrysts (up to 0.5 mm), possibly amphibole or coarser grained primary biotite, are completely altered to fine biotite. Very fine grained biotite is also abundant in the matrix. Accessory minerals include magnetite, ilmenite, titanite, zircon, apatite, and chlorite. Secondary carbonate may comprise up to 10% of the rock.

The relationship between the Deception Hill Porphyry and the surrounding greenstones is unclear as these greenstones are deeply weathered and poorly exposed. The porphyry has a SHRIMP U–Pb zircon age of 3023 ± 10 Ma (Nelson, 1999), and so cannot be related to felsic volcanic and intrusive rocks of the c. 2733 Ma Marda Complex (Pidgeon and Wilde, 1990; Nelson, in prep.). Instead, the Deception Hill Porphyry may represent a high-level equivalent of the poorly exposed felsic volcanic rocks in the Ryans Gnamma Hole area.

Metamorphosed sedimentary rocks (As, Ash, Ashd, Asi, Asq, Ass, Ac, Aci)

Metamorphosed sedimentary rocks may form a substantial part of the lower greenstone succession on JOHNSTON RANGE, but, except for the prominent ridges of BIF and chert, are rarely well exposed.

Where metasedimentary rocks are shown as undivided (*As*), they are typically deeply weathered and their identification is based on the presence of poorly preserved sedimentary textures, or their association with nearby rocks that are more clearly sedimentary.

Metamorphosed shale and minor siltstone (*Ash*) is typically black to grey but commonly weathers brown and purplish, particularly when ferruginous. Sedimentary structures are rare, and largely consist of millimetre-scale parallel laminations. Shaly units within the lower greenstone succession are commonly moderately to strongly foliated, and a weak to strong crenulation is common. The shale and siltstone consist of very fine grained, strongly aligned aggregates of sericite(–chlorite) and quartz, commonly permeated by iron oxides; graphitic shale is developed locally. In the coarser rock types, polygonized quartz may form trails parallel to the foliation.

Shaly metasedimentary rocks of the lower greenstone succession outcrop on JOHNSTON RANGE in four main areas. To the west and northwest of the Diemals Homestead, two distinctive units of shale with minor siltstone and cherty bands, up to 20 m thick, are flanked by high-Mg basalt and metagabbro. These units represent distinct marker horizons that help to define the Watch Bore Syncline. The lower shaly unit is exposed continuously on the western

limb of the syncline, but discontinuously on the eastern limb. The upper black shale unit is exposed on the eastern limb where it hosts copper mineralization at Coppermine Bore, and in the area 4.5 km south of Kim Bore (see **Base metals**). The unit has not been observed on the western limb of the syncline. The intercalation with felsic and mafic volcanic horizons and the presence of gossanous units (see **Relict units**) distinguish the metamorphosed shale and siltstone package to the north-northeast of the Clampton mine from similar lithologies of the Diemals Formation (see **Diemals Formation**). Shale units are intermittently exposed in a northeasterly trending belt to the west of Evanston mine, where they are found in association with both metabasaltic rocks and BIF. Ferruginized metamorphosed shale is in contact with felsic rocks of the Marda Complex in the area to the southeast of Pigeon Rocks (around MGA 720400E 6681000N and further to the northeast). The shale is strongly foliated and gently folded, and intercalations of BIF and jaspilitic horizons suggest that the shale here is part of the lower greenstone succession.

Foliated pelitic rocks with andalusite or staurolite, and possible cordierite (*Ashd*) outcrop southwest of the Bronzewing mine and to the southeast of Clearwaters Bore, where they are found near faulted granite–greenstone contacts. In deeply weathered rocks, identification of porphyroblasts is based on grain morphology. Bedding is defined by varying concentrations of muscovite or sericite(–chlorite), quartz, and iron oxides, and there are millimetre-sized chert clasts in the metamorphosed siltstone and very fine grained sandstone beds. Andalusite is almost always partly to completely altered to sericite and pyrophyllite. Relict andalusite porphyroblasts preserve a subidiomorphic prismatic habit with square cross sections, and are typically several millimetres long, but locally up to 3 cm long. Southeast of Clearwaters Bore, prekinematic formation of andalusite is indicated by reorientation and wrapping of the foliation around the porphyroblasts. However, in the Bronzewing area, andalusite growth post-dates the main foliation and a second weak foliation can be seen locally to crosscut the andalusite grains at a high angle. Near Ryans Gnamma Hole, diamond drilling of the pelites and associated gossanous horizons for base-metal exploration during the 1970s indicated the presence of iron-rich garnet, chloritoid, biotite, corundum, hercynite, iron-rich amphibole (cummingtonite–grunerite), tourmaline, and possibly anthophyllite (Dennis, 1979). Around Clearwaters Bore (MGA 739300E 6722300N), pelitic schist outcrops include andalusite–biotite–quartz schist and garnet–chlorite–quartz schist. The mineral assemblages of these pelites and their restriction to the vicinity of a granite–greenstone contact, supports growth of the observed metamorphic phases during contact metamorphism under locally developed, upper greenschist facies conditions (see **Metamorphism**).

Deeply weathered and typically ferruginized, fine-grained metasedimentary rocks (*Asi*) are characteristically preserved on the flanks of chert and BIF ridges, and are most common to the southwest and west of the Diemals Homestead. They are composed of metamorphosed shale and siltstone with interleaved chert and BIF, and are typically deeply weathered and poorly exposed.

Quartz-rich metasedimentary rock (*Asq*) forms a distinct unit near the exposed top of the succession that can be traced from west of Pigeon Rocks, through the Yokradine Hills and Die Hardy Range, to the area east of Deception Hill (see **Stratigraphy, Lower greenstone succession**). The metasedimentary rocks include quartzite and chert, with quartzite the most abundant rock type. The quartzite is typically very clean, with quartz strained, flattened, and sutured at grain contacts. In some instances, the quartzite represents a relatively well-sorted sandstone with well-defined beds, up to 0.5 m thick, which range from fine to medium grained. Elsewhere the quartzite represents fine- to coarse-grained, poorly sorted sandstone. In a well-exposed section in a fold hinge southwest of Pigeon Rocks (MGA 716200E 6685400N), some of the very fine grained, quartz-rich metasedimentary rocks contain very fine opaque grains, possibly iron oxides, which, along with grain-size variations, define laminae and thinly bedded units up to 3 mm thick. These rocks also contain microscale graded bedding, and macroscale truncations and troughs where they have been eroded by the deposition of overlying coarse, poorly sorted sandstone, now quartzite. Pinch-and-swell structures (Fig. 5) and possible scours and troughs are visible in some outcrops. These structures, along with locally exposed cross-beds in the clean quartzite, indicate westwards younging, which suggests that the quartz-rich metasedimentary rocks are near the top of the exposed part of the succession in this area.

Quartz-rich metasedimentary rock (*Asq*) in a poorly exposed area east of Deception Hill (between the northeastern part of the Die Hardy Range and the Bullfinch–Evanston Road) contains local pyritic intervals (e.g. MGA 734300E 6694500N). In this area, the quartzites are typically clean, fine to coarse grained, and thinly bedded to laminated. The coarser varieties are texturally immature, with fine to coarse, angular, very poorly sorted quartz grains set in clay-rich matrix (e.g. MGA 731700E 6695300N). Quartz is strained and grain boundaries are sutured.

Metamorphosed sandstone (*Ass*) is confined to a small outcrop in the Broad Bents area. It consists of poorly sorted, subrounded quartz and chert clasts up to 2 mm across. The groundmass is ferruginized and strongly deformed, consisting of recrystallized quartz and minor clay minerals.

Metamorphosed BIF and ferruginous banded chert (*Aci*) forms prominent ridges in two areas. In the north they outline the Watch Bore Syncline, and Horse Well and Diemals Anticlines (Figs 3 and 4), whereas in the southeast they form the Die Hardy Range and Yokradine Hills. The BIF is a typically steel-grey to blue, black and locally red (jaspilitic), laminated rock with alternating laminae of quartz and magnetite or hematite. Individual laminae range from less than 0.05 mm to greater than 1 mm thick with sets of laminae, defined by iron-oxide content, that range from less than 1 mm to greater than 1 cm thick. Quartz is typically recrystallized but may be microcrystalline where the rock has been subjected to only low-grade metamorphism. Other metamorphic minerals that may be present in low-grade metamorphosed BIF include muscovite, stilpnomelane, and apatite (e.g. on the

SW125 21.02.01

Figure 5. Pinch-and-swell structures in quartz-rich metasedimentary rock southwest of Pigeon Rocks (MGA 716200E 6685400N)

western side of the Yokradine Hills, northeast of Pigeon Rocks, at MGA 727200E 6690300N). Where it has undergone higher grade metamorphism, BIF and ferruginous chert may contain grunerite (e.g. northeast of Pigeon Rocks at MGA 723300E 6692500N), clinopyroxene (e.g. in drill cuttings north of Mount Geraldine at MGA 733200E 6683000N), and biotite (e.g. in drill cuttings on the eastern side of the Die Hardy Range at MGA 732700E 6683700N). Apart from bedding, few sedimentary structures are preserved. Broken slabs and sheets of ferruginous chert in the Yokradine Hills contain small-amplitude ripple marks (MGA 727100E 6687000N). Beds and layers within units of BIF and ferruginous chert (*Aci*) are commonly brecciated or complexly folded. While some of these features are due to large-scale deformation, it is likely that others are due to local deformation of partly consolidated sediments.

A very coarse, iron-cemented breccia unit outcrops on the eastern side of the main ridge of the Die Hardy Range, northeast of the Redlegs prospect (around MGA 728500E 6689000N). This unit, which forms an apron that can be traced for about 1 km along the side of the ridge, probably represents an ancient depositional surface. However, its absolute age is uncertain and it has been included with lateritic duricrust (*Rf*). Similar, less well-exposed aprons of cemented BIF and chert breccia flank other parts of the Die Hardy Range and Yokradine Hills.

Metamorphosed chert (*Ac*) consists of laminated to very thinly bedded (i.e. from <1 mm to 1 cm) quartz, now recrystallized. The layering is defined by variations in grain size (very fine to fine grained) of the recrystallized quartz, and by variations in the content of fine iron oxides. Where deformed (e.g. the unit east of the Die Hardy Range), quartz grains are strained, flattened, and sutured.

Upper greenstone succession

Marda Complex (AfMd, AfMf, AfMi, AfMiy, AfMsh, AfMshd, AfMr, AfMv)

The Marda Complex comprises metamorphosed, acid to intermediate, extrusive and intrusive volcanic rocks and associated metasedimentary rocks. Rocks of the Marda Complex outcrop over an area of about 700 km^2, mainly in the northern part of Jackson (Fig. 2; Hallberg et al., 1976; Taylor and Hallberg, 1977; Riganti and Chen, 2000; Riganti et al., 2000), and are poorly exposed in the southern part of Johnston Range, with outcrops confined to the area southeast of Pigeon Rocks.

Metamorphosed dacitic rocks of the Marda Complex (*AfMd*) contain plagioclase as idiomorphic phenocrysts and glomeroporphyritic aggregates up to 4 mm, set in a fine-grained quartzofeldspathic matrix with accessory opaque oxides. Locally abundant amygdales are up to 4 mm long and subrounded to ellipsoidal. They are commonly filled by granoblastic quartz with minor chlorite and, less commonly, by sericite, calcite, and siderite. Iron-rich chlorite, sericite, and carbonate overprint the primary assemblage. Small biotite flakes and fine, granular opaque oxides define a weak to moderate

foliation. Fine-grained micaceous, schistose intercalations may represent either a more strongly deformed equivalent of the metadacite or thin volcaniclastic horizons.

Strongly deformed, deeply weathered rock near the northern edge of the Marda Complex (*AfMf*) was probably a mixed package of felsic volcanic and volcaniclastic rocks, with sedimentary intervals including shale and siltstone. A small unit of strongly foliated felsic rocks in the northwest (MGA 700600E 6733200N), 5 km west-southwest of Grass Flat Bore, is almost certainly unrelated to the Marda Complex, but is probably a very strongly deformed felsic igneous or metasedimentary unit within the lower greenstone sequence.

Metamorphosed andesitic rocks of the Marda Complex outcrop on the southern edge of JOHNSTON RANGE, just west of the Bullfinch–Evanston Road. They include massive andesite and basaltic andesite (*AfMi*), now altered to very fine grained, amphibole- and plagioclase-bearing rocks, locally with sericitic veins, in which little primary texture is preserved. Amygdaloidal andesites (*AfMiy*) are characterized by abundant large (up to 3 cm, although typically smaller), quartz-filled amygdales and plagioclase phenocrysts up to 5 mm. Calcite and subordinate siderite are locally abundant in amygdales, and there is local carbonate alteration.

Foliated pelite of the Marda Complex (*AfMsh*) outcrops on the southern edge of JOHNSTON RANGE. An area of weathered pelitic schist containing numerous relict porphyroblasts (*AfMshd*), assigned to the Marda Complex, lies just west of the Bullfinch–Evanston Road (MGA 729500E 6679200N). The porphyroblasts are mostly altered, but square and prismatic outlines suggest that they may have been originally andalusite. It is possible that some of the grains may have been staurolite. The porphyroblastic pelite is cut by a prominent, strongly foliated siliceous unit that is interpreted as a quartz vein.

Metamorphosed rhyolitic rocks of the Marda Complex (*AfMr*) are generally fine grained, massive to strongly foliated, and pale grey to cream in colour. The groundmass has been recrystallized into a granoblastic assemblage dominated by quartz with minor muscovite and sericite. Poikilitic andalusite porphyroblasts are common but vary considerably in abundance. The rhyolite is associated with small, fine-grained, muscovite-bearing quartzite and weakly crenulated, quartz–mica schist horizons. These units typically occupy low-lying areas between the more-massive rhyolitic outcrops and very likely represent volcaniclastic beds. Sparse andalusite porphyroblasts, commonly retrograded to pyrophyllite, poikilitically enclose polygonized quartz, but are also wrapped around by the foliation. This suggests that the metamorphism is due to the intrusion of the nearby Pigeon Rocks Monzogranite, and pre-dates at least the major D_3 regional deformation event (see **Structural geology** and **Metamorphism**).

At the northernmost end of the rhyolite exposures, a small outcrop of conglomerate (MGA 726120E 6682580N) is dominated by angular clasts of banded and ferruginous chert (varying in size from a few millimetres up to 5 cm) and millimetre-sized, rounded quartz clasts in a fine-grained, quartz-rich cement. Dark-grey shale and fine-grained, ferruginized sandstone flank the conglomerate to the north. Larger outcrops of a similar conglomerate are exposed near the base of the Marda Complex on JACKSON (Fig. 2; Riganti and Chen, 2000, in prep.).

Metamorphosed, fine-grained felsic volcanic rocks of the Marda Complex (*AfMv*) include a range of rock types that cannot be separated at the map scale. They comprise foliated, feldspar-phyric or featureless rhyolite, commonly deeply weathered; and very fine grained, brown to black and white, thinly banded felsic tuffaceous units, locally displaying intraformational gentle to tight folds and brecciation. Quartz–muscovite schists identical to those described above are subordinate.

Diemals Formation (Ae, Aec, Aeh, Aehd, Ael, Aeq, Aes, Aesf, Aesp)

The Diemals Formation is a clastic metasedimentary succession exposed in the central-western part of JOHNSTON RANGE, where it fills a roughly triangular basin approximately 40 km long and up to 15 km wide. It rests unconformably on metamorphosed sedimentary and mafic igneous rocks of the lower greenstone succession (see **Stratigraphy**).

Undifferentiated metasedimentary rocks of the Diemals Formation (*Ae*) include poorly exposed, deeply weathered, and locally ferruginized pelite, siltstone, and sandstone in which sedimentary structures have been largely obliterated.

Metamorphosed silty argillite and subordinate, fine-grained sandstone (*Aeh*) form the lowermost recognizable unit of the Diemals Formation, and are best exposed about 9 km west to northwest of Deception Hill, and in an area extending from the Yarbu mine to east of the Bullseye mine. In the latter area, the absence of gossanous horizons, chert, and BIF intercalations, as well as the lack of felsic volcanic and tuffaceous beds, were used to distinguish the metasedimentary rocks of the Diemals Formation from similarly fine-grained rocks of the lower greenstone succession (see **Metamorphosed felsic rocks** and **Metamorphosed sedimentary rocks**). The contact between the greenstones and the Diemals Formation is not exposed in the Yarbu–Bullseye area, but appears to be broadly conformable to the south of Ryans Gnamma Hole.

Silty argillite in the lower part of the Diemals Formation is fawn to yellow–brown and grey to black in colour, with common purple weathering, and is characterized by layers with various amounts of quartz, sericite, and iron oxides. The thickness of individual beds ranges from a few centimetres up to 80 cm, but is typically less than 15 cm. The contacts between beds are commonly sharp. Common sedimentary structures include rhythmic layering (typically on a scale of a few millimetres to a few centimetres), graded and cross-bedding (locally indicating overturning of the sequence, e.g. at MGA 706600E 6693630N), as well as less common parallel laminations. Liesegang banding is widespread at a number of localities, and can hinder recognition of primary sedimentary features.

Fine-grained metasedimentary rocks equivalent to those described above, but characterized by abundant andalusite porphyroblasts (*Aehd*), are found adjacent to the faulted granite–greenstone contact west of the Yarbu workings. Andalusite crystals range from a few millimetres up to 8 cm in the thicker beds, and petrographic investigations indicate pre- to syn-kinematic crystal growth. In addition to andalusite, staurolite and cordierite were also identified at a few localities, their occurrence resticted to compositionally suitable layers. Chlorite schist horizons (*Ael*), which are intercalated with andalusite-bearing pelite (e.g. at MGA 705070E 6691630N), consist of fine-grained chlorite (probably after amphibole), minor biotite and feldspar, detrital quartz, and accessory opaque oxides and titanite. These intercalations represent sediments with a considerable mafic input, indicating erosion from a greenstone basement at the onset of deposition of the Diemals Formation.

Lenses of metamorphosed polymictic conglomerate with minor sandstone (*Aec*) are intercalated with silty argillite and pebbly sandstone, 9 km northwest of Deception Hill. The conglomerate is clast supported, with a ferruginous and quartz-rich, sandy to silty matrix. Rounded to subangular clasts range in size from a few centimetres up to 40 cm, and are variably flattened depending on their lithology. Clasts of reworked sandstone and argillite are dominant, but there are also clasts of banded chert, BIF, and weathered mafic rocks. Quartz, granitoid, and felsic porphyry clasts are locally abundant, whereas weathered clasts of amygdaloidal, possibly basic to intermediate rocks are rare. In general, the clasts are similar in composition to greenstones exposed to the east. Some chert and BIF boulders display tight to isoclinal folding (Fig. 6), indicating that the greenstone sequence from which these clasts are derived was deformed prior to deposition of the Diemals Formation. Some of the reworked sandstone clasts are composite and contain lithic fragments of chert and sandstone. Sedimentary structures within the conglomerate lenses are mainly confined to sandstone intercalations and include normal grading, parallel laminations, and local cross-bedding; scour troughs are also present. The contact of some conglomeratic lenses with the underlying pelites appears to be gradational, with a progressive decrease in thickness of conglomeratic beds and size of clasts from east to west.

Metamorphosed sandstone (*Aes*) is typically a massive to well-bedded, medium- to coarse-grained quartz–feldspar rock, with minor siltstone and local pebbly to conglomeratic intercalations. Graded bedding, cross-bedding, and scour troughs are developed locally. The dominant rock types include quartz and lithic greywacke, ferruginous sandstone, and more-mature quartz arenite, and, locally, quartzite. The poorly sorted quartz greywacke is characterized by subangular to subrounded, monocrystalline and polygonized quartz grains with subordinate chert clasts in the core of the Yarbu Syncline, which are supported by a clay- and sericite-rich matrix. Sporadic quartz grains with embayed outlines may be volcanic in origin. Lithic greywacke contains more abundant chert fragments and very fine grained, turbid brown clasts, possibly derived from mafic volcanic rocks. In the more ferruginous varieties, the sandstone matrix is permeated by iron oxides, which also infiltrate quartz and chert clasts along grain boundaries and fractures. More-mature quartz arenites are distinguished by an assemblage of sutured, commonly monocrystalline quartz grains with subordinate

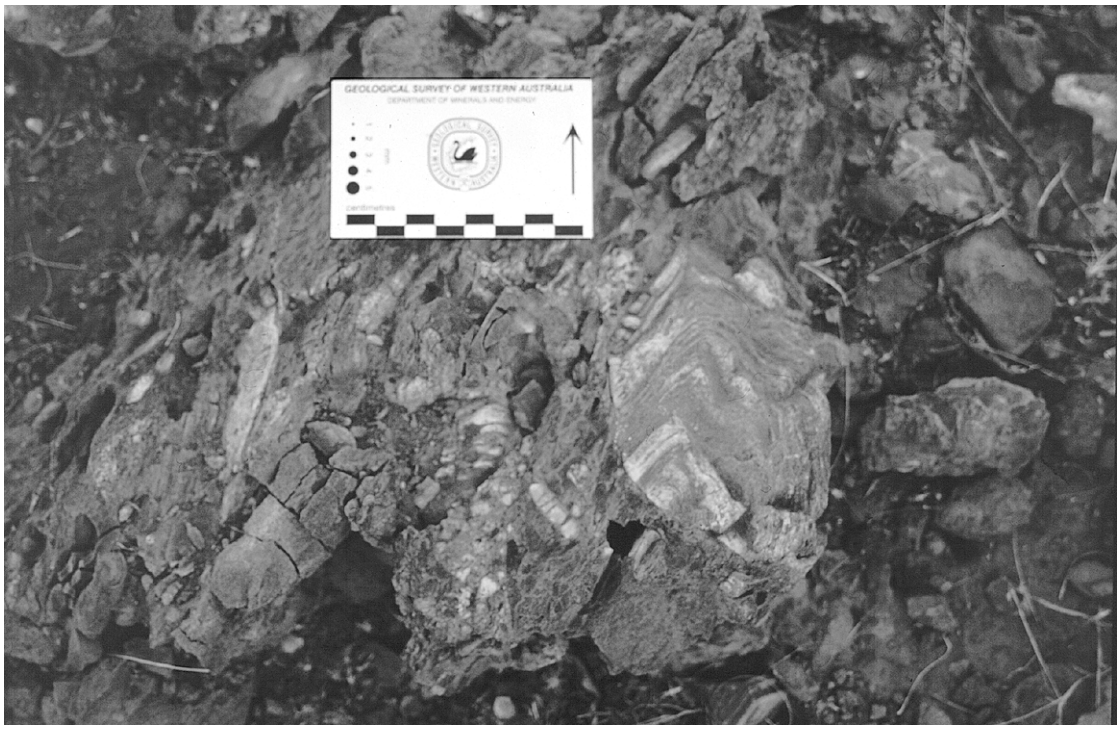

SW126 21.02.01

Figure 6. Conglomerate in the Diemals Formation (MGA 717472E 6699839N)

chert fragments. Interstices are filled with sericite and muscovite. Poikiloblastic andalusite grains have developed around quartz grains locally. Strongly foliated sandstone (*Aesf*) adjacent to the Clampton Fault is characterized by flattening of quartz grains, which have pronounced undulose extinction, and are wrapped around by the feldspar- and clay-rich matrix. Cataclasis in pressure shadows is relatively common.

Metamorphosed pebbly sandstone (*Aesp*) is characterized by sparse to abundant, subangular to subrounded clasts of vein quartz, black chert, black-and-white-banded cherts, as well as some BIF and black shaly fragments in a quartz-rich, sandy matrix. Clasts are commonly a few centimetres across, but can be up to 20 cm. Monomictic (banded chert) to polymictic conglomeratic beds with chert and quartz fragments up to 20 cm across form intercalations within the pebbly sandstone (e.g. near the Yarbu Syncline core at MGA 711140E 6693550N and MGA 711360E 6689970N). Clasts in the pebbly sandstone above the unconformity south of Kim Bore are dominated by vein quartz.

Quartzite and quartz-rich metasandstone (*Aeq*) and strongly foliated metasandstone (*Aesf*) are exposed locally to the west of Kim Bore. The quartzite is massive to well bedded, and consists mainly of quartz with subordinate muscovite.

Mafic gneiss (*Anb*)

Mafic gneiss (*Anb*) is found only in the lower sections of shallow mineral-exploration drillholes, and in waste dumps from old shafts near the Clampton mine (MGA 703580E 6685030N). It is fine grained and dark, with fine, irregular bands dominated by biotite or actinolite, which alternate with plagioclase-rich bands that may contain quartz. Apatite and sphene are abundant accessory phases; local vesuvianite and minor opaque oxides are also present. Zircon is identified by abundant pleochroic halos within biotite flakes. The texture and mineralogical assemblage of this rock suggest recrystallization and pervasive metasomatism of a mafic protolith during synkinematic intrusion of nearby granite.

Granitoid rocks (*Ag, Agf, Agm, Agmf, Agn, Agpi*)

Granitoid rocks occupy extensive areas around, and locally within, the greenstone successions on Johnston Range. They are typically poorly exposed and commonly weathered. Outcropping granitoids range in composition from monzogranite to granodiorite, with monzogranite by far the most abundant variety.

Undivided granitoid rock (*Ag*) is either too deeply weathered to allow identification of the original composition, or outcrops in areas for which no compositional data are available. Strongly foliated granitoid rocks (*Agf*), whose original composition cannot be determined, are shown separately.

Fresh outcrops of massive (*Agm*) and foliated (*Agmf*) monzogranite are widespread on Johnston Range, but even the massive varieties show some degree of strain and metamorphic recrystallization. Monzogranite may be fine to coarse grained, equigranular to porphyritic, and always contains biotite as a primary phase. Minor opaque oxides, mainly magnetite, are locally altered to goethite. Muscovite may be a primary and secondary constituent, and biotite is locally replaced by chlorite. Plagioclase is commonly zoned, and porphyritic monzogranite may contain phenocrysts of K-feldspar greater than 5 mm across. Strongly foliated, fine- to medium-grained leucocratic monzogranite is exposed to the west of the Clampton Fault (Fig. 3). Biotite content and grain size can vary considerably, and compositional banding is developed locally (e.g. near Old Stone Well at MGA 699920E 6684580N). Aplite and pegmatite veins commonly crosscut the monzogranite at various angles, but appear to be foliated in the same orientation. Later quartz veins, ranging in thickness up to 30 m, are commonly undeformed. The age of this granitoid could not be determined. Undeformed monzogranite from about 45 km west of Kim Bore on Ross has a SHRIMP U–Pb zircon age of 2656 ± 8 Ma (Nelson, in prep.), but its relationship with other granitoids in the region is unknown.

Fresh monzogranite (*Agm*) at Olby Rock is equigranular and weakly to moderately deformed with the foliation defined by the alignment of biotite and diffuse, folded mafic schlieren. Accessory minerals include euhedral magnetite, apatite, titanite, allanite, fluorite, and chlorite after biotite. This rock has a SHRIMP U–Pb zircon age of 2697 ± 8 Ma (Nelson, 1999). This age is similar to those commonly obtained for other examples of granitoid rocks that make up the extensive areas between greenstone belts in this region (Nelson, 2000, in prep.). However, strongly deformed monzogranite in the Evanston Shear Zone on Lake Giles to the east has a SHRIMP U–Pb zircon age of 2654 ± 6 Ma (Nelson, in prep.; see **Structural geology**).

The Pigeon Rocks Monzogranite (*Agpi*) is typically a medium-grained biotite monzogranite in which quartz is strained and strongly recrystallized, and plagioclase is commonly zoned. Accessory minerals include apatite, titanite, zircon, fluorite, and opaque oxides. Common secondary minerals include epidote and sericite or muscovite. Plagioclase is commonly saussuritized, and biotite commonly altered to chlorite (Nelson, 1999). On the southeastern side of Pigeon Rocks (MGA 720000E 6687500N), typical monzogranite contains angular enclaves of grey, plagioclase-phyric, biotite-rich microgranite. The Pigeon Rocks Monzogranite (*Agpi*) has a contact-parallel foliation that is more pronounced near granite–greenstone contacts. The SHRIMP U–Pb zircon age of 2729 ± 4 Ma (Nelson, 1999) for the monzogranite is within error of the age of the c. 2733 Ma Marda Complex (Pidgeon and Wilde, 1990; Nelson, in prep.) and the c. 2730 Ma Butcher Bird Monzogranite to the south on Jackson (Nelson, in prep.; Riganti and Chen, in prep.).

The distinct, sharp, plug-like outline of the Pigeon Rocks Monzogranite (*Agpi*) on aeromagnetic images; the presence of a contact-parallel foliation near the margins of the intrusion that dips steeply towards the greenstones; and the presence of downdip lineations, including

striations and mineral lineations in greenstones adjacent to granite–greenstone contacts, suggest that the present disposition of the Pigeon Rocks Monzogranite is at least partly due to diapiric intrusion.

Veins and dykes (*q, g*)

Quartz veins (*q*) are abundant on JOHNSTON RANGE and are represented on the map where they form prominent topographic ridges or clear airphoto lineaments. They have been emplaced at various times during the deformation of the granite–greenstones, but no absolute ages have been determined. Veins typically consist of massive, milky quartz, but early-emplaced veins may be strongly deformed. Some massive veins clearly intrude fractures that are assigned to the latest east–west compressional event recognized in the region (see **Structural geology**).

Fine-grained granitoid veins and dykes (*g*) within the greenstones typically intruded near granite–greenstone contacts and parallel to the structural grain. They are compositionally similar to the major granitoid intrusions, and are probably apophyses from these bodies.

Mafic dykes (*Pdy*)

There are several prominent easterly and northeasterly trending magnetic features on JOHNSTON RANGE (Fig. 4) that have been interpreted as mafic dykes. These are the latest identified Precambrian features in the region, but there are no known outcrops on JOHNSTON RANGE. Hallberg (1987), in a review of available data concerning mafic and ultramafic dykes of the Yilgarn Craton, concluded that those in the central part of the craton were probably emplaced along tensional fractures between c. 2400 and 2000 Ma.

Stratigraphy

There are two distinct greenstone successions on JOHNSTON RANGE — a lower mafic-dominated succession, and an upper succession (Marda Complex and Diemals Formation) that includes clastic and felsic volcanic and volcaniclastic rocks (Hallberg et al., 1976; Chin and Smith, 1983; Walker and Blight, 1983; Griffin, 1990). A locally tectonized unconformity between the lower succession and clastic rocks of the Diemals Formation is preserved in the area south of Kim Bore. The lower succession has undergone a significantly more-complex deformation history than the upper succession (see **Structural geology**). Limited geochronological data, such as the SHRIMP U–Pb zircon age of 3023 ± 10 Ma (Nelson, 1999) for the Deception Hill Porphyry, indicate that the lower greenstone succession is substantially older than the upper succession, where a SHRIMP U–Pb zircon determination on detrital zircons in the Diemals Formation on JOHNSTON RANGE gives a maximum depositional age of 2729 ± 9 Ma (Nelson, in prep.), and SHRIMP U–Pb zircon determinations on felsic volcanic rocks of the Marda Complex on JACKSON give an age of c. 2733 Ma (Pidgeon and Wilde, 1990; Nelson, in prep.).

Lower greenstone succession

No formal stratigraphy has been defined for the lower greenstone succession. The first-generation 1:250 000-scale mapping of Chin and Smith (1983) and Walker and Blight (1983) suggested a single-cycle stratigraphy with the lowermost unit recognized being a metamorphosed quartz arenite (not seen on JOHNSTON RANGE), overlain by a sequence consisting of ultramafic-dominated, mafic-dominated, and then metasedimentary-dominated rocks. Most of the BIF is contained within the middle part of the sequence, which also contains substantial mafic and ultramafic rocks. Dalstra (1995) presented descriptions of stratigraphy from various parts of the region, notably the Diemals area, but did not attempt a detailed regional correlation. In these Explanatory Notes, the lower succession has been divided into three informal stratigraphic associations, in the sense used by Hallberg (1985) for the Laverton–Leonora region to the east. The subdivision here is based on the recognition of distinct lithological groupings, and correlation of various rock types in relation to the major units of BIF in the Marda–Diemals region. Subsequent mapping may allow a more formal definition of the regional stratigraphy.

Unfortunately, the age of the lower greenstone succession is not absolutely constrained by the c. 3023 Ma age of the Deception Hill Porphyry, as this is an isolated outcrop and its relationship to the rest of the succession is unclear. The only clearly felsic volcanic rocks that formed within the lower greenstone succession on JOHNSTON RANGE are some tuffaceous beds near Ryans Gnamma Hole. However, they are too poorly exposed and weathered to be suitable for SHRIMP dating, and the lithological association in this area is difficult to relate to those exposed in the rest of the sheet area. The only other constraint on the age of the lower greenstone succession is a maximum depositional age of c. 3300 Ma for quartzites at the base of the exposed greenstone sequence in the Illaara greenstone belt to the east (Wyche, 1999; Nelson, 2000).

The most complete section of the lower greenstone succession on JOHNSTON RANGE is the Diemals stratigraphy, preserved in a pair of faulted anticlines south and west of Diemals Homestead (the Diemals and Horse Well Anticlines), and in the Watch Bore Syncline farther to the west (Fig. 3). Data obtained from this area during the current mapping program have allowed the lower greenstone succession to be divided into the three broad associations referred to above (Fig. 7a). The lowermost association consists mainly of mafic and minor ultramafic rocks. The middle association is characterized by BIF, chert, and clastic sedimentary rocks (extensively intruded by gabbro), and includes abundant high-Mg basalt towards the top. The uppermost association contains at least two extensive shale horizons (one a black shale with local copper mineralization), which are intercalated with gabbro sills. Thick units of high-Mg basalt, also intercalated with gabbro, mark the top of the exposed sequence.

Exposure is typically poor elsewhere on JOHNSTON RANGE, and stratigraphic sections are commonly disrupted by complex deformation. Incomplete stratigraphic sections

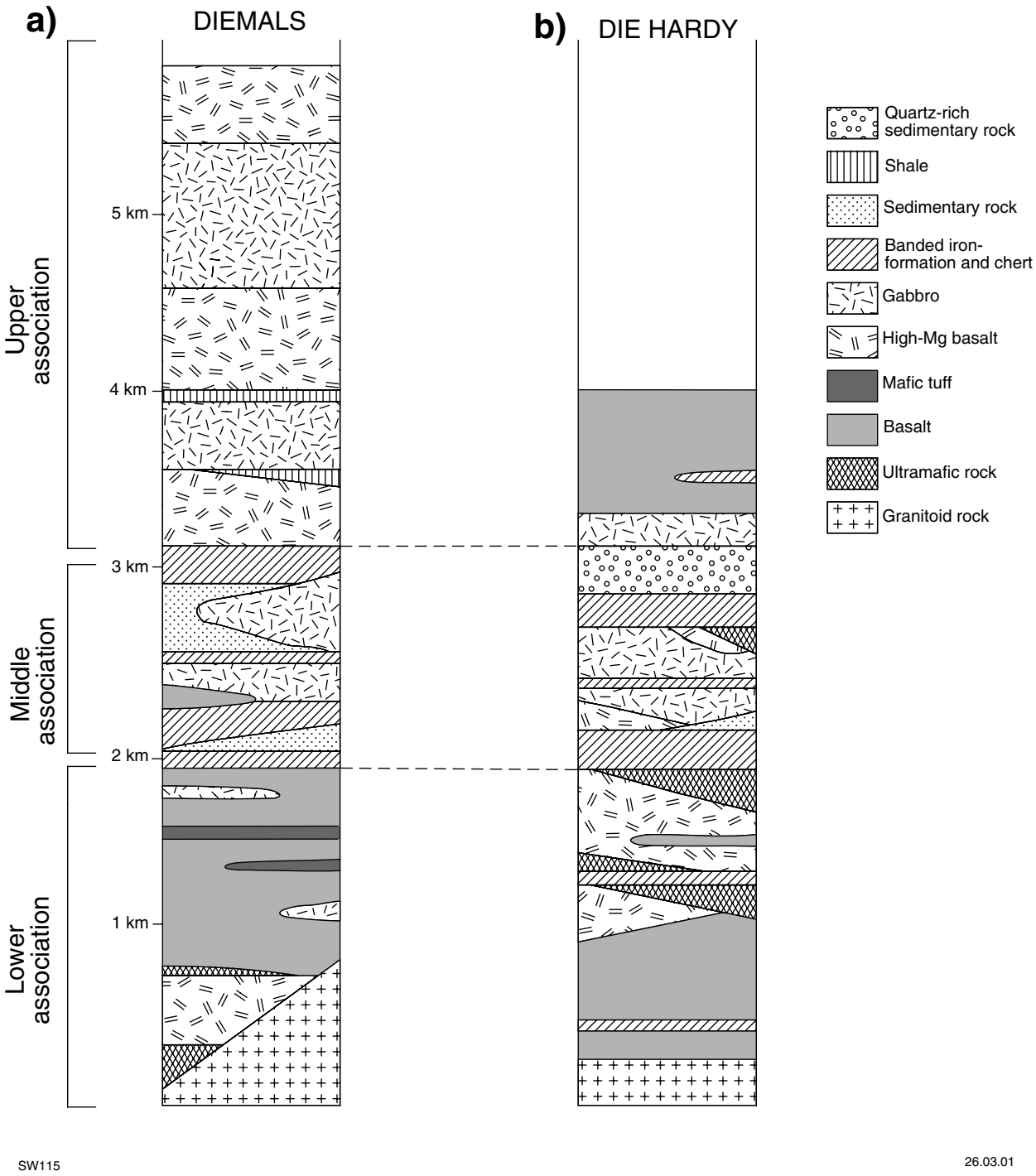

Figure 7. Stratigraphic relationships in the lower greenstone succession on JOHNSTON RANGE

are exposed in the Broad Bents antiform (Fig. 3), and in the Die Hardy Range (Figs 1 and 3).

The Broad Bents stratigraphy is not only poorly exposed, but also complicated by a possible large-scale, refolded fold (see **Structural geology**). The preserved section consists of a prominent unit of ultramafic cumulate within a dominantly mafic sequence, overlain by one or two units of BIF, and associated mafic volcanic and shaly metasedimentary rocks.

The Die Hardy stratigraphy (Fig. 7b) is based on sections in the Die Hardy Range – Pigeon Rocks region, which are locally well exposed, but also structurally complex. If the prominent BIF ridges in this area are correlated with the prominent BIF units in the Diemals area, then there are some differences between the stratigraphic successions in the two areas. The presence of clastic sedimentary rocks immediately above the uppermost of the main ridge-forming units of BIF suggest that the succession on the western side of Pigeon Rocks

is the same as that in the Yokradine Hills, Die Hardy Range, and in the hills west of the Bullfinch–Evanston Road.

Only the lower and middle associations of the lower greenstone succession are recognized in the Die Hardy stratigraphy. The lowest exposed part of the lower association is an interval of fine- to medium-grained mafic rocks containing a thin chert horizon. A thin BIF unit higher in the succession is associated with high-Mg basalt and ultramafic schist. The interval between the thin BIF unit and the first major regional BIF unit appears to be dominated by high-Mg basalt and ultramafic schist. The middle association consists of two prominent BIF units and chert separated by a unit of clinopyroxene-rich gabbro that, in the northern and northeastern Die Hardy Range area, contains a thin, disrupted horizon of BIF. An extensive clastic sedimentary unit with locally preserved sedimentary structures, such as cross-beds and graded bedding, overlain by gabbro, marks the top of this part of the succession. Areas of BIF and mafic rocks east of Deception Hill may be part of the upper association, but the area is structurally complex and relationships are unclear.

A comparison of the Diemals and Die Hardy stratigraphies shows a broad similarity between the lower two associations. However, the upper associations are quite different with the upper part of the Diemals stratigraphy dominated by high-Mg basalt and gabbro, and that of the Die Hardy stratigraphy characterized by the presence of clastic sedimentary rocks. Thus a direct correlation of the two successions implies that either the part of the upper association directly above the uppermost major BIF unit has been removed from one of the sections, or that the upper part of each of the successions represents a quite distinctly different geological environment, and possibly a different depositional basin.

Upper greenstone succession

The U–Pb zircon geochronological data suggest that rocks of the Marda Complex and Diemals Formation are broadly contemporaneous. However, lack of continuous exposure and probable lateral facies variations make it difficult to establish a clear stratigraphic succession. The Marda Complex is only locally exposed in the southern part of JOHNSTON RANGE, with the main exposure farther south on JACKSON (Riganti and Chen, 2000). The contact between the lower greenstone succession and the Marda Complex is marked locally by black shale and conglomerate (see **Marda Complex**), but this contact is better exposed to the south on JACKSON (Riganti and Chen, in prep.).

The Diemals Formation fills a roughly triangular basin about 40 km long and up to 15 km wide. It comprises polymictic conglomerate, pebbly sandstone, siltstone, argillite, and minor quartzite that are typically metamorphosed to lower greenschist facies, with higher grades adjacent to the granite–greenstone contact. The formation was formally defined by Walker and Blight (1983), but has now been extended further south to include fine-grained metasedimentary rocks that outcrop southeast of the Clampton mine and in the northern part of JACKSON (Riganti and Chen, 2000). The area occupied by the Diemals Formation is largely fault-bounded, and the sequence has been folded into the regional-scale, westerly verging, moderately northerly plunging Yarbu Syncline. The formation can be subdivided into a lower and an upper sequence, best exposed in the limbs and core of the syncline respectively. The lower sequence on the western limb consists of silty argillite with minor chloritic schist and graphitic shale near the base. On the eastern limb, the lowermost exposed part of the formation consists of conglomerate lenses interbedded with siltstone, argillite, and pebbly sandstone. The upper sequence, exposed in the core of the syncline, consists of pebbly sandstone and sandstone. Medium-scale folding and poor exposure prevent an accurate evaluation of the total thickness of the Diemals Formation. A maximum age for the deposition of the Diemals Formation is given by detrital zircons from a sandstone bed near the syncline core, which yielded a SHRIMP U–Pb age of 2729 ± 9 Ma (Nelson, in prep.).

The Diemals Formation unconformably overlies the mafic-dominated lower greenstone succession. The unconformity is best exposed 5 km south of Kim Bore, where a poorly sorted conglomerate contains clasts of black shale and deeply weathered (?mafic) rocks, typically 3–15 cm across, which are derived from the underlying greenstones. At this locality, the basal conglomerate and overlying sandstone dip moderately to the south and south-southwest, whereas the underlying greenstones, particularly the black shale unit, dip steeply to the west-southwest.

Field characteristics and facies relationships suggest that the Diemals Formation was deposited in a fluviatile to lacustrine environment over a deformed greenstone basement. The asymmetric distribution of sedimentary facies and grain-size variation in the lower part of the formation suggests that the sediments were transported predominantly from east to west, and that they were derived mainly from the uplift and erosion of the lower greenstone succession to the east, with some contributions from granitoid sources to the west. The latter source dominated during deposition of the upper part of the formation (Riganti et al., 2000). The presence of intraformational sandstone clasts within the conglomerate indicates an active tectonic environment during deposition.

Structural geology

Several deformation schemes have been proposed for the Marda–Diemals region (Chin and Smith, 1983; Walker and Blight, 1983; Griffin, 1990; Dalstra, 1995; Dalstra et al., 1999; Greenfield and Chen, 1999; Chen et al., 2001), with most schemes recognizing an early layer-parallel deformation in the lower greenstone succession. The deposition of the upper greenstone succession was followed by, and probably partly contemporaneous with, broadly east–west compression resulting in the development of northerly trending, upright folding and the development of north-northeasterly to north-northwesterly trending, ductile shear zones. A subsequent episode of

east–west to east-northeast – west-southwest compression produced conjugate sets of mainly brittle north-north-easterly and east-southeasterly faults and fractures.

Early deformation (D_1)

Recent SHRIMP U–Pb zircon geochronology (Nelson, 1999, in prep.) does not support the suggestion of Walker and Blight (1983) that compositional layering and gneissic foliation represents the earliest identifiable deformation. Limited data suggest that the gneissic foliation has developed in rocks that are younger than the lower greenstone succession — for example, gneissic granitoid at Yacke Yackine Dam on JACKSON has a SHRIMP age of c. 2711 Ma (Nelson, in prep.). As the lower succession had already been deformed before deposition of the Diemals Formation after c. 2729 Ma, the gneissic foliation must be due to a later event.

The earliest recognized deformation (D_1) structures on JOHNSTON RANGE are layer-parallel, tight to isoclinal folds (Walker and Blight, 1983; Griffin, 1990; Dalstra, 1995; Dalstra et al., 1999; Greenfield and Chen, 1999). These structures are most readily recognized in units of BIF. They have been mapped in the hinge areas of the Horse Well and Diemals Anticlines (Fig. 3) where they have wavelengths of up to 300 m. Smaller-scale D_1 folds have been recognized in other parts of the sheet — for example, in the Yokradine Hills (MGA 725400E 6684500N) and near the Evanston mine (MGA 740200E 6705800N). At the Evanston mine locality, isoclinal D_1 folds have been refolded around an open D_2 fold hinge, and there is local development of sheath folds. The present orientation of D_1 structures suggests that they have developed in a north–south compressional regime. Evidence of early deformation is preserved locally in other parts of the succession. For example, an early schistosity in tremolite–chlorite schist on the western side of the Yokradine Hills (MGA 725600E 6691500N) has been refolded about a small-scale, open D_2 antiform (Fig. 8). However, exposures are commonly of such poor quality that these features are rarely seen.

The timing of the early deformation is unclear. However, it must pre-date the deposition of the Diemals Formation after 2729 ± 9 Ma (Nelson, in prep.) because conglomerate of the Diemals Formation contains clasts of folded BIF, and the unconformity between the lower greenstone succession and the Diemals Formation has not been affected by this deformation.

East–west compression (D_2–D_3)

The present-day configuration of the granitoids and greenstones is the result of a prolonged period of east–west compression. This deformation has been recognized and described by a number of workers (Libby et al., 1991; Dalstra, 1995; Dalstra et al., 1999; Greenfield and Chen, 1999; Chen et al., 2001), but the sequence and timing of events is still poorly understood. Recently acquired U–Pb SHRIMP zircon geochronology data (Dalstra et al., 1998; Nelson, 1999, 2000, in prep.; Qiu et al., 1999) have

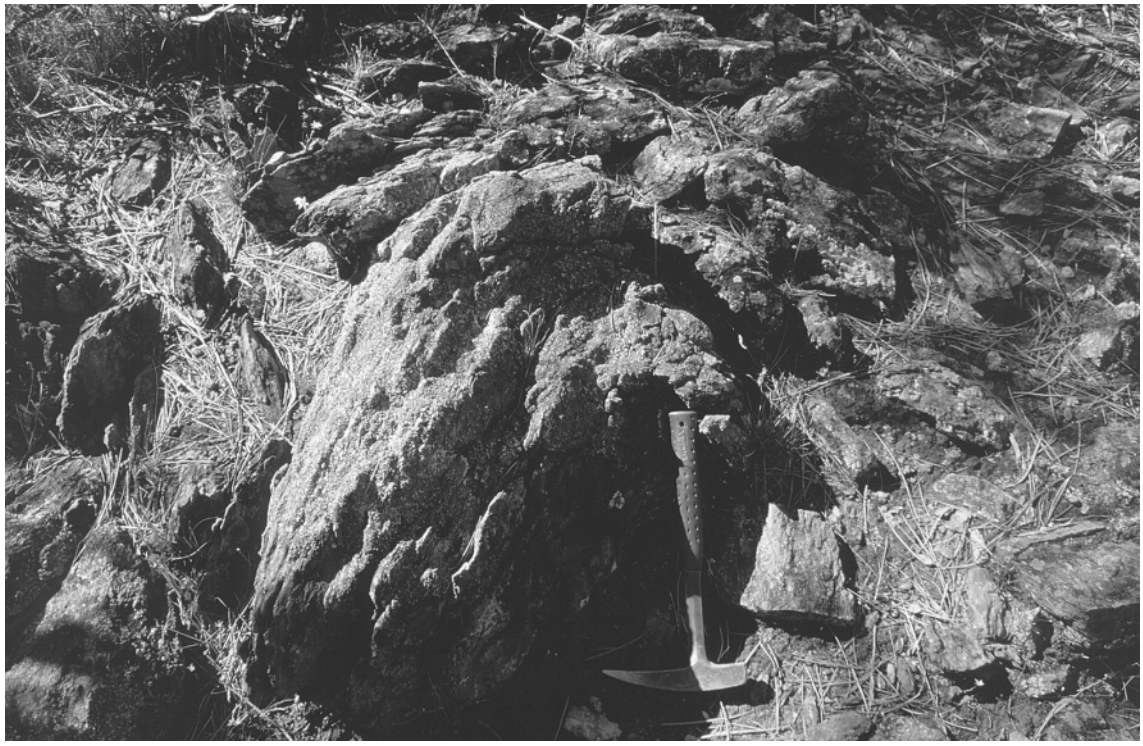

SW127 21.02.01

Figure 8. Folded tremolite–chlorite schist north of the Yokradine Hills with a small-scale D_2 fold that folds early (?D_1) schistosity (MGA 725600E 6691500N)

SW128 21.02.01

Figure 9. Regional-scale, northerly plunging D_2 anticline north of the Redlegs prospect. The photograph has been taken from a ridge of BIF on the western limb of the anticline. The BIF unit on the eastern limb of the anticline can be seen in the middle distance (photo taken towards the northeast from MGA 7728600E 6690900N)

provided some constraints on the duration of the deformation episode.

In the Marda–Diemals region, structures attributed to D_2–D_3 include northeasterly to northwesterly trending, open to tight folds (Figs 9 and 10), and northeasterly to northwesterly trending faults and ductile shear zones (Figs 2, 3, and 4). The timing of the initiation of the east–west compression is not clear, but it was probably active at least during the emplacement of the Marda Complex and associated granitoids, including the Pigeon Rocks Monzogranite, and the deposition of the Diemals Formation at 2.73 Ga (Pidgeon and Wilde, 1990; Nelson, 1999, in prep.). The increasing amount of geochronological data on granitoid and felsic volcanic rocks in the central and western parts of the Yilgarn Craton (Pidgeon and Wilde, 1990; Wiedenbeck and Watkins, 1993; Pidgeon and Hallberg, 2000; Nelson, in prep.) indicates widespread felsic magmatism that post-dates the older greenstones, but stretches back to at least 2.81 Ga. If this magmatic activity is associated with the developing east–west compressional regime, then this may have been a very long-lived, Yilgarn-wide deformation event.

On Johnston Range, the earliest D_2–D_3 structures include the open, upright, shallowly plunging folds such as the Diemals and Horse Well Anticlines, and the Watch Bore Syncline. Some of these regional-scale folds are overprinted by large-scale shear zones and faults. Thus, although the evolution of these structures is not always clear, these folds have been assigned to D_2.

East–west compression also coincided with a major period of granitoid intrusion around 2.69 Ga in the Marda–Diemals area. Bloem et al. (1997) and Dalstra et al. (1998) mapped regional structural patterns and analysed pressure–temperature (P–T) data from both granitoids and adjacent greenstones in the Ghooli complex, south of Johnston Range on the Jackson and Southern Cross 1:250 000 sheets, which indicated that these granitoids were emplaced as nested diapirs. They argued that the granitoids in this region crystallized at c. 2690 Ma and remained hot and deep until the onset of the east–west compression at c. 2636 Ma, which coincided with the diapiric rise of the granitoids. However, SHRIMP data on a range of granitoids and gneissic granitoids in the Southern Cross and Marda–Diemals area suggest that the period of granitoid intrusion was long-lived, at least as old as 2.77 Ga (Mueller and McNaughton, 2000), broadly coincident with the syn-D_2 felsic volcanism, and contemporaneous with felsic magmatism in the Murchison Province (Wiedenbeck and Watkins, 1993). In the Marda–Diemals area, the earliest time constraint on D_2–D_3 is the development of a gneissic fabric in granitoid rocks with a SHRIMP U–Pb zircon age of 2711 ± 4 Ma at Yacke Yackine on Jackson (Nelson, in prep.; Riganti and Chen, in prep.).

According to Chen et al. (2001), the presence of broad areas of granitoids produced regional rheological inhomogeneities that markedly affected the regional patterns produced by the ongoing compression. During this continued deformation, large rigid granitoid bodies

SW129 21.02.01

Figure 10. Mesoscale, southerly plunging D_2 fold in the Die Hardy Range (MGA 728400E 6687300N)

impinged on the greenstones and reoriented the earlier D_2 structures to produce large-scale, arcuate structures bounded by regional-scale ductile shear zones (Chen et al., 2001). The ductile shear zones trend northeasterly to northwesterly, and the arcuate structures are convex towards the greenstones, concave towards the impinging granitoids, and are linked by northerly trending contractional zones. These second-generation structures within the overall D_2–D_3 east–west compressional regime are assigned to D_3. Sense of movement on the shear zones is given by features such as S–C fabrics and rotated porphyroclasts. Northeasterly trending shear zones, such as the Evanston Shear Zone (Fig. 3), have a dextral sense of movement (Greenfield, in prep.), whereas northwesterly trending shear zones, such as the Mount Dimer Shear Zone (Figs 2 and 3), have a sinistral sense of movement.

The major deformation style in the northerly trending contractional zones was flattening or, locally, reverse movement. One of these contractional zones, in the Die Hardy Range – Yokradine Hills area, consists of a set of tight, shallowly plunging, northerly trending folds, and some probable reverse faults. The folds probably developed early in the D_2 compressional phase. However, the Pigeon Rocks Monzogranite has acted as a buttress during subsequent westerly directed compressional stress, and so the folds have tightened. Continued westerly directed compression has resulted in the development of the northeasterly trending Evanston Shear Zone, the northwesterly trending Mount Dimer Shear Zone, and probable reverse faults in the Die Hardy Range area (Figs 2 and 3).

Deposition of clastic sedimentary rocks of the Diemals Formation may have continued through much of the period of D_2–D_3 deformation, with the Yarbu Syncline (Fig. 3) developing late during D_3. The last movement in D_3 may have been the development of the gentle westwardly concave curvature of the Yarbu Syncline.

A constraint on a minimum age for D_3 is provided by the SHRIMP U–Pb zircon age of 2656 ± 3 Ma on an undeformed syenogranite, which cuts the D_3 Koolyanobbing Shear Zone near Koolyanobbing, about 100 km south of the southern boundary of Johnston Range (Fig. 2; Qiu et al., 1999). However, strongly deformed monzogranite in the D_3 Evanston Shear Zone on Lake Giles (Fig. 2; Greenfield, in prep.) has a SHRIMP U–Pb zircon age of 2654 ± 6 Ma (Nelson, in prep.). If the Koolyanobbing and Evanston Shear Zones have a similar history, then D_3 ended at about 2655 Ma.

East–west to east-northeast – west-southwest compression (D_4)

The last major deformation episode prior to the emplacement of Proterozoic mafic dykes along easterly trending tension fractures (see **Mafic dykes**) was a period of east–west to east-northeast – west-southwest compression (D_4) that resulted in large-scale, conjugate sets of mainly brittle, north-northeasterly and east-southeasterly faults and fractures that are best seen on aeromagnetic images (Fig. 4). Where the displacement can be seen, it is dextral on north-northeasterly trending faults, and sinistral on south-southeasterly trending faults. These

faults and fractures cut across greenstones and granitoids, and are commonly filled by quartz veins. The absolute age of these structures is not known, but similar structures about 100 km to the east on RIVERINA cut across the c. 2632 Ma Ularring Monzogranite (Wyche, 1999; Nelson, 2000).

A late-stage, easterly trending foliation with associated crenulation and open folding has been noted in sandstone of the Diemals Formation (around MGA 707200E 6711800N and MGA 709200E 6711800 N), but its extent and relationship with other deformation events is unclear.

Metamorphism

The first regional metamorphic study to include the JOHNSTON RANGE area was that of Binns et al. (1976). A subsequent, more-detailed petrographic study of metamorphic patterns in the Southern Cross Province by Ahmat (1986) described the range of metamorphic assemblages in the various rock types, and refined the map of Binns et al. (1976). These studies demonstrated that metamorphic grade in the northern part of the Southern Cross Province is typically lower than that in the south, a feature recognized by Gee et al. (1981). They further showed that, in the northern part of the province, metamorphic grades are low to very low and strain is low in the middle of greenstone belts, and grades are low to medium and locally high with high strain adjacent to granite–greenstone belt margins.

A more-detailed study of metamorphic patterns in the Marda–Diemals region (Dalstra, 1995; Dalstra et al., 1999) included a petrographic study and detailed P–T determinations on amphibole–plagioclase pairs in metamorphosed tholeiitic mafic rocks from a number of localities on JOHNSTON RANGE and JACKSON. This study suggested a two-stage metamorphic history. It also showed that although temperatures in amphibolite-facies rocks may have been as high as 540°C, pressures were typically less than 400 MPa.

According to Dalstra et al. (1999), the prehnite–pumpellyite facies rocks, preserved mainly in and around the Marda Complex on JACKSON, retain much of their primary mineralogy, including igneous clinopyroxene. The typically very low strain and spilitization of these rocks suggest that they were metamorphosed in an oceanic basin with very high heat flow. Ahmat (1986) attributed the early, low-grade metamorphic event to burial metamorphism.

Greenschist-facies rocks are widespread and prevalent through much of the central part of JOHNSTON RANGE. Dalstra et al. (1999) differentiated low- and high-strain, greenschist-facies rocks. Low-strain rocks have little or no metamorphic fabric and basalts preserve primary igneous characteristics such as vesicles (commonly filled by chlorite, quartz, epidote, and, rarely, calcite) and varioles. In the high-strain rocks, igneous features are rarely preserved and there is a strongly developed metamorphic foliation. In mafic rocks, the metamorphic foliation is not only typically defined by tremolite–actinolite, but also by biotite and chlorite.

On JOHNSTON RANGE, amphibolite-facies rocks are restricted to within a few kilometres of granite–greenstone contacts. Mafic varieties are characterized by the presence of dark, metamorphic hornblende and may contain clinopyroxene (diopside) and garnet. More magnesian rocks typically consist of tremolite and plagioclase, and possibly magnetite. Metamorphosed BIF typically contains grunerite, and pelitic rocks commonly contain andalusite. The fact that the highest metamorphic grades are found near granite–greenstone contacts, coupled with the relatively low pressures involved in the metamorphism of these rocks, indicates that the major influence on metamorphic grade was the proximity of the rocks to the intruding granitoids. Local overprinting of metamorphic minerals by a D_2–D_3 foliation (e.g. see **Marda Complex**, where high-grade metamorphic rocks are attributed to the intrusion of the nearby Pigeon Rocks Monzogranite) and the deformation of granitoids in D_3 shear zones suggest that the peak metamorphism is syn-D_2 or earlier. However, the difference in age between emplacement times of various granitoids — for example, c. 2697 Ma for the monzogranite at Olby Rock compared with c. 2729 Ma for the Pigeon Rocks Monzogranite — implies that the attainment of highest metamorphic grades may be diachronous across the region.

The late, brittle (D_4) faults contain retrograde assemblages including chlorite, sericite, and quartz (Dalstra et al., 1999).

Cainozoic geology

Although more than 80% of JOHNSTON RANGE is covered by Cainozoic regolith deposits, there are no specific studies of the regolith in this region. Mapping of the regolith is based on field observations combined with interpretation of airphotos and Landsat TM5 images. The classification system of Hocking et al. (2001) is used, which is, in turn, based on the Residual–Erosional–Depositional (RED) scheme of Anand et al. (1993).

Relict units (*Rd, Rf, Rfc, Rf_gs_m, Rgp_g, Rqs_s, Rz, Rzu*)

Relict units typically form hills, breakaways, and broad plateaux on JOHNSTON RANGE. They probably represent the oldest elements in the Cainozoic landscape.

Undivided duricrust (*Rd*) may be either siliceous or ferruginous, and has been mapped mainly in areas underlain by granitoid rocks. Such areas are commonly covered by a veneer of sand with minor pisolitic laterite, silt, and clay (*Sl*). Clearly ferruginous or lateritic duricrust (*Rf*) forms over both granitoid and greenstone rocks, and are seen as dark red-brown tones on airphotos and false-colour Landsat images. Along the eastern side of the Die Hardy Range, this unit includes iron-cemented conglomerate containing very coarse BIF clasts. In other places, the lateritic duricrust has been partly eroded and reworked, but some remnant duricrust commonly remains. Lateritic duricrust in ridge-forming units (*Rfc*) typically represents weathered, ferruginized metasedimentary rocks.

Relict sedimentary features, such as thin bedding and lamination, suggest that these rocks may have been chert or BIF, but they may also include shale. Locally developed gossanous bands within shaly metasedimentary rock (Rf_gs_m) near Ryans Gnamma Hole consist of massive to disseminated goethitic and limonitic concentrations of variable thickness and extent (Dennis, 1979; Taylor, 1979; see **Base metals**). The largest stratiform lenses can be followed along strike for several hundred metres and are up to 20 m thick, but there are numerous smaller bodies. The gossanous bands resemble lateritic duricrust in most exposures, but derivation by supergene alteration of a sulfide-rich body is indicated by common weathered-out cubic shapes (mainly after pyrite) and locally preserved boxwork textures. Some of the lenses are weakly magnetic.

Residual quartzofeldspathic sand over granitoid rock (Rgp_g) forms around and adjacent to granitoid outcrops. Areas of residual sand may contain small patches of outcrop. Similarly, extensive areas of probably residual sandplain (Rqs_s) form a thin veneer over the quartzofeldspathic metasedimentary rocks of the Diemals Formation. In these areas, bedding trends in the underlying metasedimentary rocks are commonly visible on airphotos and satellite images. Such areas may contain local patchy outcrop.

Siliceous duricrust forms areas of silcrete (*Rz*), mainly over granitoid rocks. This may include massive, cryptocrystalline, chalcedonic material, and also the more typical variety in which quartz clasts are set in cryptocrystalline siliceous cement (Butt, 1985). Pale- to dark-brown silica caprock over ultramafic rocks (*Rzu*) commonly preserves primary igneous textures, particularly cumulate textures in former peridotite and dunite.

Depositional units (*C, Cf, Clc$_i$, Cq, W, Wf, A, Ap, Ll, L1$_d$, L$_m$, L2$_d$, S, Sl*)

Depositional regolith units are the most widely exposed surficial deposits on Johnston Range.

Undivided colluvial units (*C*) include proximal deposits of sand, silt, gravel, and coarse talus below ridges and breakaways. In places, this material consists dominantly of weathered, ferruginized rocks and reworked ferruginous duricrust (*Cf*). Where colluvium lies adjacent to prominent ridges of BIF and chert (Clc_i), these rock types make up the major component of the talus. Similarly, quartz-dominated talus adjacent to prominent quartz veins (*Cq*) is also distinguished. The quartz-rich colluvium unit also includes more distal colluvium where quartz gravel is a major component of the deposit. Such areas form distinctive light patches on airphotos and satellite images.

Areas of sheetwash (*W*) represent distal deposits, away from prominent ridges and breakaways. These deposits typically consist of sand, silt, and clay. However, sheetwash adjacent to areas of lateritic duricrust may be ferruginous, and commonly contains abundant fine, ferruginous grit. This ferruginous sheetwash (*Wf*) has a distinctive dark-reddish-brown pattern on airphotos, and can also be distinguished on satellite images.

Alluvium (*A*) includes clay, silt, sand, and gravel that has been deposited on active channels and floodplains. The limits of these areas are based on the interpretation of airphotos and satellite images. Claypans within active alluvial systems (*Ap*) are also distinguished.

Lacustrine deposits on Johnston Range comprise part of the southern end of Lake Barlee. This major lake system lies on the westerly flowing side of a large-scale, palaeodrainage watershed (Hocking and Cockbain, 1990). Lake surfaces are covered by a veneer of salt crust, commonly gypsiferous evaporite (*Ll*). Active dunes of dominantly evaporitic material within and adjacent to lake systems ($Ll1_d$) are characterized by a lack of vegetation. These have been distinguished from mixed alluvial, eolian, and lacustrine deposits (L_m). Stabilized dune areas with substantial vegetation cover ($L2_d$) represent more ancient deposits, although the true age of these deposits is unknown.

Quartz sand (*S*), which forms a layer of variable thickness over other regolith units and granitoid and greestone rocks, may be residual material derived from granitoid or metasedimentary rocks, or eolian deposits. Yellow sand over duricrust (*Sl*) contains areas of pisolitic gravel, silt, and clay. This unit displays darker tones than the quartz sand (*S*) on airphotos and false-colour satellite images, and may be a mixture of residual and eolian deposits.

Economic geology

The only mineral commodity with any significant production from Johnston Range is gold. Historical mineral production is discussed in Townsend et al. (2000).

Gold

Gold has been produced from a number of centres on Johnston Range, but the greatest production has come from the Evanston district. Gold mineralization is epigenetic, structurally controlled, and hosted by shear zones and quartz veins. At Evanston, veins containing gold are hosted by highly altered, amphibolite-facies rocks along contacts between BIF and ultramafic schists. Mafic rocks do not host significant gold mineralization (Dalstra, 1995). Gold mineralization also formed along a contact between BIF and mafic schist in the Die Hardy area. Elsewhere, gold mineralization is hosted by mafic (Diemal Find, Clampton, Bullseye) and metasedimentary rocks (Yarbu, Bronzewing). Descriptions of workings with some historical production data are given by Matheson and Miles (1947). A summary of recorded historical production is given in Appendix 3.

Thirty kilograms of silver was produced from gold mine tailings at Evanston between 1957 and 1960 (Walker and Blight, 1983).

Base metals

A thin, black-shale horizon that can be traced over a strike length of at least 10 km on the eastern limb of the Watch

Bore Syncline, from north of Coppermine Bore to south of Kim Bore, contains traces of copper mineralization. An extensive exploration program from 1966 to 1971 that included diamond drilling, rock-chip and soil sampling, and geophysical studies, failed to find any economic copper mineralization (e.g. Western Mining Corporation Ltd, 1967; Marston, 1979).

Sulfide-bearing, black-shale horizons have also been found east of Clampton mine where they are marked by gossanous caprock (see **Relict units**) within a sequence of mafic, ultramafic, and felsic volcanic and volcaniclastic rocks. The gossanous units are typically less than 10 m thick at the surface. An extensive exploration program carried out by Carpentaria Exploration Company Pty Ltd (Taylor, 1979) in search of volcanogenic massive sulfide deposits included geological mapping, rock-chip and soil sampling, geophysical studies, and rotary and diamond drilling. Most of the gossans are associated with pyritic black shale, but one drillhole intersected a massive body of pyrrhotite- and magnetite-rich rock.

Acknowledgements

The authors would like to thank Titan Resources NL for access to geophysical data, and Tony McPherson at Diemals for advice and assistance during the course of the mapping program.

References

AHMAT, A. L., 1986, Metamorphic patterns in the greenstone belts of the Southern Cross Province, Western Australia: Western Australia Geological Survey, Report 19, p. 1–21.

ANAND, R. R., CHURCHWARD, H. M., SMITH, R. E., SMITH, K., GOZZARD, J. R., CRAIG, M. A., and MUNDAY, T. J., 1993, Classification and atlas of regolith-landform mapping units: CSIRO, AMIRA Project P240A, Exploration and Mining Restricted Report 440R (unpublished).

ARNDT, N. T., and NISBET, E. G., 1982, Komatiites: London, George Allen and Unwin, 526p.

BEARD, J. S., 1990, Plant life of Western Australia: Kenthurst, N.S.W., Kangaroo Press, 319p.

BINNS, R. A., GUNTHORPE, R. J., and GROVES, D. I., 1976, Metamorphic patterns and development of greenstone belts in the eastern Yilgarn Block, Western Australia, *in* The early history of the Earth *edited by* B. F. WINDLEY: London, John Wiley and Sons, p. 303–313.

BLATCHFORD, T., and HONMAN, C. S., 1917, The geology and mineral resources of the Yilgarn Goldfield, Part III — The gold belt north of Southern Cross, including Westonia: Western Australia Geological Survey, Bulletin 71, 321p.

BLOEM, E. J. M., DALSTRA, H. J., RIDLEY, J. R., and GROVES, D. I., 1997, Granitoid diapirism during protracted tectonism in an Archaean granitoid–greenstone belt, Yilgarn Block, Western Australia: Precambrian Research, v. 85, p. 147–171.

BUTT, C. R. M., 1985, Granite weathering and silcrete formation on the Yilgarn Block, Western Australia: Australian Journal of Earth Sciences, v. 32, p. 415–432.

CAS, R. A. F., and WRIGHT, J. V., 1987, Volcanic successions, modern and ancient — a geological approach to processes, products and successions: London, Allen and Unwin, 528p.

CHEN, S. F., LIBBY, J. W., GREENFIELD, J. E., WYCHE, S., and RIGANTI, A., 2001, Geometry and kinematics of large arcuate structures formed by impingement of rigid granitoids into greenstone belts during progressive shortening: Geology, v. 29, p. 283–286.

CHIN, R. J., and SMITH, R. A., 1983, Jackson, W.A.: Western Australia Geological Survey, 1:250 000 Geological Series Explanatory Notes, 30p.

DALSTRA, H. J., 1995, Metamorphic and structural evolution of the greenstone belts of the Southern Cross – Diemals region of the Yilgarn Block, Western Australia, and its relationship to the gold mineralisation: University of Western Australia, PhD thesis (unpublished).

DALSTRA, H. J., BLOEM, E. J. M., RIDLEY, J. R., and GROVES, D. I., 1998, Diapirism synchronous with regional deformation and gold mineralisation, a new concept for granitoid emplacement in the Southern Cross Province, Western Australia: Geologie en Mijnbouw, v. 76, p. 321–338.

DALSTRA, H. J., RIDLEY, J. R., BLOEM, E. J. M., and GROVES, D. I., 1999, Metamorphic evolution of the central Southern Cross Province, Yilgarn Craton, Western Australia: Australian Journal of Earth Sciences, v. 46, p. 765–784.

DENNIS, R. W., 1979, Petrography and model of mineralization for the Clampton Prospect, Yilgarn Goldfield, Western Australia, Technical report no. 739; Carpentaria Exploration Company Pty Ltd: Western Australia Geological Survey, Statutory mineral exploration report, Item 2561 (unpublished).

GEE, R. D., BAXTER, J. L., WILDE, S. A., and WILLIAMS, I. R., 1981, Crustal development in the Yilgarn Block, *in* Archaean geology *edited by* J. E. GLOVER and D. I. GROVES: Geological Society of Australia (W.A. Division); 2nd International Archaean Symposium, Perth, W.A., 1980, Proceedings, Special Publication, no. 7, p. 43–56.

GILES, E., 1889 (reprinted 1995), Australia twice traversed: Perth, Western Australia, Hesperian Press, 382p.

GREENFIELD, J. E., in prep., Geology of the Lake Giles 1:100 000 sheet: Western Australia Geological Survey, 1:100 000 Geological Series Explanatory Notes.

GREENFIELD, J. E., and CHEN, S. F., 1999., Structural evolution of the Marda–Diemals area, Southern Cross Province: Western Australia Geological Survey, Annual Review 1998–99, p. 68–73.

GRIFFIN, T. J., 1990, Southern Cross Province, *in* Geology and mineral resources of Western Australia: Western Australia Geological Survey, Memoir 3, p. 60–77.

HALLBERG, J. A., 1985, Geology and mineral deposits of the Leonora–Laverton area, northeastern Yilgarn Block, Western Australia: Perth, Western Australia, Hesperian Press, 140p.

HALLBERG, J. A., 1987, Postcratonization mafic and ultramafic dykes of the Yilgarn Block: Australian Journal of Earth Sciences, v. 34, p. 135–149.

HALLBERG, J. A., JOHNSTON, C., and BYE, S. M., 1976, The Archaean Marda igneous complex, Western Australia: Precambrian Research, v. 3, p. 111–136.

HOCKING, R. M., and COCKBAIN, A. E., 1990, Regolith, *in* Geology and mineral resources of Western Australia: Western Australia Geological Survey, Memoir 3, p. 591–602.

HOCKING, R. M., LANGFORD, R. L., THORNE, A. M., SANDERS, A. J., MORRIS, P. A., STRONG, C. A., and GOZZARD, J. R., 2001, A classification system for regolith in Western Australia: Western Australia Geological Survey, Record 2001/4, 22p.

LIBBY, J., GROVES, D. I., and VEARNCOMBE, J. R., 1991, The nature and tectonic significance of the crustal-scale Koolyanobbing shear zone, Yilgarn Craton, Western Australia: Australian Journal of Earth Sciences, v. 38, p. 229–245.

MARSTON, R. J., 1979, Diemals prospect, *in* Copper mineralization in Western Australia: Western Australia Geological Survey, Mineral Resources Bulletin 13, p. 128.

MATHESON, R. S., and MILES, K. R., 1947, The mining groups of the Yilgarn Goldfield north of the Great Eastern Railway: Western Australia Geological Survey, Bulletin 101, 242p.

MUELLER, A. G., and McNAUGHTON, N. J., 2000, U–Pb ages constraining batholith emplacement, contact metamorphism, and the formation of gold and W–Mo skarns in the Southern Cross area, Yilgarn Craton, Western Australia: Economic Geology, v. 95, p. 1231–1258.

NELSON, D. R., 1999, Compilation of geochronology data, 1998: Western Australia Geological Survey, Record 1999/2, 222p.

NELSON, D. R., 2000, Compilation of geochronology data, 1999: Western Australia Geological Survey, Record 2000/2, 251p.

NELSON, D. R., in prep., Compilation of geochronology data, 2000: Western Australia Geological Survey, Record.

PIDGEON, R. T., and HALLBERG, J. A., 2000, Age relationships in supracrustal sequences in the northern part of the Murchison Terrane, Archaean Yilgarn Craton, Western Australia: a combined field and zircon U–Pb study: Australian Journal of Earth Sciences, v. 47, p. 153–165.

PIDGEON, R. T., and WILDE, S. A., 1990, The distribution of 3.0 Ga and 2.7 Ga volcanic episodes in the Yilgarn Craton of Western Australia: Precambrian Research, v. 48, p. 309–325.

QIU, Y. M., McNAUGHTON, N. J., GROVES, D. I., and DALSTRA, H. J., 1999, Ages of internal granitoids in the Southern Cross region, Yilgarn Craton, Western Australia, and their crustal evolution and tectonic implications: Australian Journal of Earth Sciences, v. 46, p. 971–981.

RIGANTI, A., and CHEN, S. F., 2000, Jackson, W.A. Sheet 2737: Western Australia Geological Survey, 1:100 000 Geological Series.

RIGANTI, A., and CHEN, S. F., in prep., Geology of the Jackson 1:100 000 sheet: Western Australia Geological Survey, 1:100 000 Geological Series Explanatory Notes.

RIGANTI, A., CHEN, S. F., WYCHE, S., and GREENFIELD, J. E., 2000, Late Archaean volcanism and sedimentation in the central Yilgarn Craton, *in* GSWA 2000 extended abstracts: Geological data for WA explorers in the new millennium: Western Australia Geological Survey, Record 2000/8, p. 4–6.

TALBOT, H. W. B., 1912, Geological investigations into the country lying between latitude 28°and 29°45' south and 118°15' and 120°40' east, embracing portions of the North Coolgardie and Murchison Goldfields: Western Australia Geological Survey, Bulletin 45, 61p.

TAYLOR, S. R., and HALLBERG, J. A., 1977, Rare-earth elements in the Marda calc-alkaline suite: an Archaean geochemical analogue of Andean-type volcanism: Geochimica et Cosmochimica Acta, v. 41, p. 1125–1129.

TAYLOR, T., 1979, Final report, Clampton prospect, Yilgarn Goldfield, Western Australia, Technical report no. 757; Carpentaria Exploration Company Pty Ltd: Western Australia Geological Survey, Statutory mineral exploration report, Item 2561, A20313 (unpublished).

TOWNSEND, D. B., GAO MAI, and MORGAN, W. R., 2000, Mines and mineral deposits of Western Australia: digital extract from MINEDEX — an explanatory note: Western Australia Geological Survey, Record 2000/13, 28p.

WALKER, I. W., and BLIGHT, D. F., 1983, Barlee, W.A.: Western Australia Geological Survey, 1:250 000 Geological Series Explanatory Notes, 22p.

WANG, Q., SCHIOTTE, L., and CAMPBELL, I. H., 1996, Geochronological constraints on the age of komatiites and nickel mineralisation in the Lake Johnston greenstone belt, Yilgarn Craton, Western Australia: Australian Journal of Earth Sciences, v. 43, p. 381–385.

WESTERN MINING CORPORATION LTD, 1967, Diemals Find base metals exploration, Annual Report TR 70/03848: Western Australia Geological Survey, Statutory mineral exploration report, Item 374, A1191 (unpublished).

WIEDENBECK, M., and WATKINS, K. P., 1993, A time scale for granitoid emplacement in the Archean Murchison Province, Western Australia, by single zircon geochronology: Precambrian Research, v. 61, p. 1–26.

WOODWARD, H. P., 1912, A general description of the northern portion of the Yilgarn Goldfield and the southern portion of the North Coolgardie Goldfield: Western Australia Geological Survey, Bulletin 46, 23p.

WYCHE, S., 1999, Geology of the Mulline and Riverina 1:100 000 sheets: Western Australia Geological Survey, 1:100 000 Geological Series Explanatory Notes, 28p.

Appendix 1

Gazetteer of localities on JOHNSTON RANGE

Locality	MGA coordinates	
	Easting	Northing
Broad Bents	740200	6716000
Bronzewing mine	707100	6691900
Bullseye mine	703600	6679600
Clampton mine	703700	6685200
Clearwaters Bore	739100	6722900
Coppermine Bore	708400	6721400
Deception Hill	725600	6696100
Die Hardy mine	731400	6682900
Diemal Find	722800	6715900
Diemals Homestead	723000	6715800
Evanston mine	740200	6706900
Grass Flat Bore	705300	6734300
Gwendolyn mine	735800	6710900
Kim Bore	709300	6717900
Mount Geraldine	732800	6682400
Olby Rock	736200	6683200
Old Stone Well	700000	6684600
Pigeon Rocks	719500	6687500
Redlegs prospect	730600	6687500
Ryans Gnamma Hole	706300	6686300
Watch Bore	706900	6728400
Yarbu mine	707200	6692700

Appendix 2

Whole-rock geochemical data from JOHNSTON RANGE

GSWA sample	*143285*	*143286*	*143287*	*143288*	*143289*	*143290*	*143291*
Rock type	*Mafic tuff*	*Basalt*	*Basalt*	*Peridotite*	*High-Mg basalt*	*Gabbro*	*Basalt*
Locality	*Diemals Homestead*	*Diemals Homestead*	*North of Deception Hill*	*North of Deception Hill*	*North of Deception Hill*	*Clearwaters Bore*	*Clearwaters Bore*
Easting	*723300*	*723300*	*724700*	*725300*	*722900*	*738700*	*738100*
Northing	*6714100*	*6714000*	*6705600*	*6705400*	*6703100*	*6722300*	*6722400*
				Percentage			
SiO_2	50.57	50.98	51.30	51.80	52.26	52.54	53.68
TiO_2	0.47	0.67	0.54	0.36	0.50	0.51	0.68
Al_2O_3	14.69	14.76	14.55	5.94	9.34	14.11	13.60
Fe_2O_3	1.71	1.77	1.99	1.36	1.29	1.48	1.73
FeO	8.47	8.64	7.97	7.78	8.39	8.25	6.78
MnO	0.18	0.18	0.18	0.19	0.19	0.15	0.20
MgO	8.44	7.65	8.00	17.75	13.58	8.08	8.23
CaO	10.66	11.40	11.35	10.35	10.89	11.16	11.88
Na_2O	2.16	1.49	1.56	0.31	0.86	1.58	1.93
K_2O	0.32	0.21	0.18	0.02	0.07	0.47	0.09
P_2O_5	0.04	0.07	0.05	0.03	0.04	0.05	0.06
S	0.01	0.00	0.01	0.01	0.01	0.01	0.00
CO_2	0.04	0.05	0.04	0.04	0.07	0.07	0.08
H_2O-	0.19	0.21	0.25	0.27	0.25	0.15	0.25
H_2O+	2.49	2.37	2.36	3.95	3.15	1.69	1.25
Fe_2O_3(Total)	11.13	11.37	10.84	10.00	10.61	10.65	9.26
Total	**100.44**	**100.44**	**100.32**	**100.16**	**100.90**	**100.29**	**100.43**
				Parts per million			
Sc	46	42	46	52	52	56	50
V	197	208	202	163	189	263	231
Cr	306	262	328	2 392	1 583	77	465
Ni	148	136	130	372	264	107	133
Cu	83	84	93	34	63	104	42
Zn	78	81	76	62	69	68	82
Ga	12	13	12	6	9	13	12
Ge	2	1	1	2	2	2	2
As	<0.3	<0.3	<0.2	<0.2	<0.2	<0.3	<0.3
Se	0.1	<0.1	0.2	<0.1	<0.1	<0.1	0.2
Br	0	0	1	0	0	0	0
Rb	10	4	4	1	2	16	1
Sr	114	86	82	12	39	71	104
Y	17	21	18	11	16	16	16
Zr	27	45	37	18	29	38	46
Nb	2	2	2	2	2	2	3
Mo	0.4	0.6	0.8	0.6	0.6	0.8	1.5
Ag	0.4	0.3	0.5	0.3	0.4	0.4	0.4
Cd	0.2	0.2	0.1	0.2	0.3	0.3	<0.1
In	<0.1	<0.1	<0.1	<0.1	<0.1	<0.1	<0.1
Sn	0.6	1.1	0.5	0.1	<0.1	0.4	0.5
Sb	<0.1	<0.1	<0.1	<0.1	<0.1	<0.1	<0.1
Te	<0.2	<0.2	<0.2	<0.2	<0.2	<0.2	<0.2
I	<0.3	<0.3	<0.3	<0.3	<0.3	<0.3	<0.3
Cs	<0.5	<0.5	<0.5	<0.5	<0.5	0.4	0.4
Ba	62	69	46	12	28	63	22
La	3	3	3	3	2	2	3
Ce	2	5	7	3	3	3	4
Nd	1.8	2.0	1.9	<1.9	<1.9	3.2	1.7
Hf	2.7	2.6	2.0	2.4	3.3	4.0	4.1
Tl	0.3	<0.4	<0.3	<0.3	<0.3	0.4	0.3
Pb	2	2	1	1	2	5	6
Bi	0.5	<0.3	0.9	0.2	<0.3	0.5	0.3
Th	0.2	0.7	0.4	0.0	0.3	0.6	0.7
U	0.1	0.4	0.5	0.3	0.3	0.4	0.2
La	1.67	–	–	2.00	2.10	–	–
Ce	3.84	–	–	4.44	5.09	–	–
Pr	0.558	–	–	0.646	0.778	–	–
Nd	2.618	–	–	2.891	3.615	–	–
Sm	0.951	–	–	0.869	1.163	–	–
Eu	0.386	–	–	0.329	0.441	–	–
Gd	1.533	–	–	1.183	1.612	–	–
Tb	0.311	–	–	0.224	0.309	–	–
Dy	2.41	–	–	1.62	2.27	–	–
Ho	0.570	–	–	0.368	0.528	–	–
Er	1.78	–	–	1.11	1.60	–	–
Tm	0.287	–	–	0.176	0.253	–	–
Yb	1.879	–	–	1.136	1.662	–	–
Lu	0.296	–	–	0.183	0.263	–	–

Appendix 2 (continued)

GSWA sample	*143369*	*143370*	*143371*	*143372*	*143373*	*143374*	*143375*
Rock type	*Gabbro*	*Gabbro*	*Basalt*	*Gabbro*	*Gabbro*	*High-Mg basalt*	*Monzogranite*
Locality	*Grass Flat Bore*	*Grass Flat Bore*	*Grass Flat Bore*	*Grass Flat Bore*	*Coppermine Bore*	*Coppermine Bore*	*West of Kim Bore*
Easting	*705600*	*705400*	*705300*	*705200*	*708500*	*708300*	*701600*
Northing	*6732600*	*6732600*	*6732600*	*6732500*	*6721600*	*6721500*	*6717600*
				Percentage			
SiO_2	51.62	52.99	54.18	50.78	51.88	51.82	75.23
TiO_2	1.00	0.66	0.80	0.47	0.94	0.70	0.12
Al_2O_3	13.54	13.48	13.70	15.64	13.79	11.73	13.46
Fe_2O_3	1.93	0.81	1.32	1.01	1.77	1.27	0.39
FeO	9.62	7.39	6.78	6.85	9.27	9.53	0.94
MnO	0.19	0.14	0.17	0.14	0.16	0.17	0.04
MgO	6.97	9.70	7.81	8.84	6.86	10.96	0.17
CaO	11.40	10.04	10.82	13.13	10.83	9.54	0.77
Na_2O	2.15	2.70	3.32	1.57	2.64	1.21	3.69
K_2O	0.11	0.46	0.11	0.09	0.14	0.10	4.99
P_2O_5	0.08	0.07	0.01	0.05	0.04	0.07	0.05
S	0.00	0.00	0.00	0.01	0.00	0.01	0.00
CO_2	0.04	0.05	0.06	0.10	0.08	0.03	0.04
H_2O-	0.18	0.11	0.11	0.18	0.31	0.22	0.13
H_2O+	1.35	1.91	1.13	1.51	1.21	2.83	0.34
Fe_2O_3(Total)	12.62	9.03	8.86	8.62	12.07	11.86	1.44
Total	**100.18**	**100.52**	**100.32**	**100.36**	**99.92**	**100.19**	**100.34**
				Parts per million			
Sc	52	46	48	42	51	42	5
V	318	244	291	187	312	244	5
Cr	97	519	278	664	82	669	4
Ni	85	141	65	101	79	175	1
Cu	17	11	1	53	3	88	2
Zn	73	48	75	53	46	83	31
Ga	14	13	15	13	14	13	19
Ge	2	2	2	2	2	2	2
As	2.5	<0.3	<0.3	1.4	3.7	<0.3	<0.5
Se	0.3	<0.1	<0.1	0.3	<0.2	0.1	<0.1
Br	1	1	0	1	0	1	0
Rb	2	19	1	3	2	1	394
Sr	89	119	80	69	111	46	48
Y	23	18	26	13	20	19	29
Zr	46	52	68	31	48	60	99
Nb	3	3	3	2	3	3	22
Mo	1.3	0.3	0.6	0.7	0.5	0.7	<0.3
Ag	0.7	0.4	0.4	<0.1	0.6	0.5	<0.1
Cd	0.5	<0.1	0.2	0.2	<0.1	0.3	<0.1
In	<0.1	<0.1	<0.1	<0.1	<0.1	<0.1	<0.1
Sn	0.5	0.4	0.3	<0.1	0.4	0.5	5.7
Sb	<0.1	<0.1	<0.1	<0.1	<0.1	<0.1	<0.1
Te	<0.2	<0.2	<0.2	<0.2	<0.2	<0.2	<0.2
I	<0.3	<0.3	<0.3	<0.3	<0.3	<0.3	<0.3
Cs	<0.5	<0.5	0.5	<0.5	0.6	<0.5	10.1
Ba	29	58	30	29	44	107	353
La	3	5	4	3	1	3	31
Ce	4	9	8	4	3	7	67
Nd	3.2	<2	2.4	<1.9	1.8	3.4	20.6
Hf	4.9	5.0	4.9	2.6	5.2	5.6	6.1
Tl	0.4	<0.3	<0.3	<0.3	0.3	0.4	2.0
Pb	2	3	3	3	1	3	47
Bi	<0.3	<0.3	0.4	<0.3	0.3	0.5	<0.3
Th	<0.5	1.1	2.0	0.5	0.4	1.0	34.9
U	0.1	0.0	0.7	0.3	0.2	0.4	11.9
La	2.64	3.94	3.68	–	–	2.66	–
Ce	7.17	9.20	8.72	–	–	6.85	–
Pr	1.263	1.247	1.363	–	–	0.977	–
Nd	6.444	5.471	6.361	–	–	4.374	–
Sm	2.156	1.699	2.233	–	–	1.531	–
Eu	0.768	0.634	0.624	–	–	0.568	–
Gd	2.888	2.247	3.065	–	–	2.089	–
Tb	0.518	0.413	0.583	–	–	0.405	–
Dy	3.58	2.86	4.11	–	–	2.89	–
Ho	0.780	0.630	0.903	–	–	0.639	–
Er	2.33	1.83	2.61	–	–	1.87	–
Tm	0.351	0.275	0.394	–	–	0.288	–
Yb	2.206	1.748	2.461	–	–	1.816	–
Lu	0.356	0.265	0.371	–	–	0.274	–

Appendix 2 (continued)

GSWA sample	*143376*	*143377*	*153299*	*153300*	*159301*	*159302*	*156281*
Rock type	*Mafic tuff*	*Mafic tuff*	*Amphibolite*	*Gabbro*	*Gabbro*	*Gabbro*	*Basalt*
Locality	*Diemals Homestead*	*Diemals Homestead*	*Bullseye mine*	*Bullseye mine*	*Bullseye mine*	*Bullseye mine*	*Deception Hill*
Easting	*722900*	*723000*	*703700*	*704200*	*704200*	*704300*	*728200*
Northing	*6714500*	*6714000*	*6680400*	*6681200*	*6681200*	*6681200*	*6698900*
				Percentage			
SiO_2	52.43	56.11	54.84	53.47	52.96	53.00	49.29
TiO_2	0.49	0.47	0.71	0.66	0.67	0.62	1.21
Al_2O_3	12.80	12.10	15.13	14.65	14.56	14.38	15.04
Fe_2O_3	2.10	2.82	1.32	2.35	1.33	1.48	2.33
FeO	7.24	5.60	7.33	6.97	7.71	8.08	9.57
MnO	0.19	0.18	0.19	0.14	0.16	0.14	0.16
MgO	9.02	6.55	6.34	7.42	7.66	8.35	6.44
CaO	9.80	12.59	11.30	9.31	11.63	9.43	11.87
Na_2O	1.27	0.38	2.11	3.55	2.10	2.30	2.11
K_2O	0.17	0.24	0.13	0.16	0.11	0.15	0.08
P_2O_5	0.05	0.05	0.06	0.07	0.07	0.06	0.07
S	0.00	0.01	0.00	0.01	0.00	0.00	0.01
CO_2	1.63	1.05	0.04	0.07	0.08	0.06	0.03
H_2O-	0.21	0.15	0.15	0.15	0.17	0.21	0.11
H_2O+	3.15	2.12	1.03	1.43	1.21	2.02	1.52
Fe_2O_3(Total)	10.14	9.04	9.46	10.09	9.89	10.45	12.96
Total	**100.53**	**100.41**	**100.68**	**100.39**	**100.41**	**100.28**	**99.81**
				Parts per million			
Sc	41	41	45	43	45	49	42
V	181	177	213	201	216	219	305
Cr	358	270	166	274	251	400	110
Ni	128	92	92	107	98	138	69
Cu	66	85	8	65	40	62	65
Zn	87	59	67	42	65	80	73
Ga	12	13	14	13	12	12	28
Ge	2	2	1	2	1	1	2
As	1.8	3.6	3.9	1.3	13.3	2.3	<0.3
Se	<0.1	<0.1	<0.1	0.2	<0.1	<0.1	<0.2
Br	0	0	0	0	0	0	<0.2
Rb	4	5	2	3	1	3	3
Sr	66	90	123	126	77	127	293
Y	17	16	17	16	18	14	27
Zr	34	33	61	59	58	52	64
Nb	2	2	3	3	3	3	4
Mo	0.4	0.7	0.7	0.3	0.5	0.7	1.0
Ag	0.3	<0.1	<0.1	<0.1	<0.1	0.4	0.5
Cd	0.2	0.4	0.3	0.1	0.3	<0.1	0.5
In	<0.1	<0.1	<0.1	<0.1	<0.1	<0.1	<0.1
Sn	0.4	0.4	0.6	0.5	0.8	0.5	1.1
Sb	<0.1	<0.1	4.1	4.3	3.0	1.4	<0.1
Te	<0.2	<0.2	<0.2	<0.2	<0.2	<0.2	<0.2
I	<0.3	<0.3	<0.3	<0.3	<0.3	<0.3	<0.4
Cs	<0.6	<0.6	<0.5	0.4	0.3	<0.5	<0.5
Ba	75	105	50	43	28	33	245
La	3	3	5	2	4	2	5
Ce	7	4	13	5	12	4	12
Nd	2.5	2.2	<1.9	2.0	2.2	<1.9	10.6
Hf	4.5	1.3	4.5	4.2	4.6	2.4	<0.1
Tl	0.5	<0.3	<0.3	0.4	<0.3	0.3	<0.6
Pb	3	3	3	3	4	4	1
Bi	<0.3	<0.3	<0.3	0.4	0.4	<0.3	<0.3
Th	0.6	0.7	2.3	2.2	2.3	1.4	<0.7
U	0.0	0.0	0.9	0.2	0.2	0.0	<0.5
La	3	.20	2.91	–	–	–	–
Ce	6.77	6	.40	–	–	–	–
Pr	0.999	0.887	–	–	–	–	–
Nd	4.373	3.895	–	–	–	–	–
Sm	1.273	1.145	–	–	–	–	–
Eu	0.515	0.474	–	–	–	–	–
Gd	1.728	1.615	–	–	–	–	–
Tb	0.325	0.303	–	–	–	–	–
Dy	2.39	2.20	–	–	–	–	–
Ho	0.559	0.510	–	–	–	–	–
Er	1.70	1.63	–	–	–	–	–
Tm	0.272	0.259	–	–	–	–	–
Yb	1.765	1.681	–	–	–	–	–
Lu	0.278	0.277	–	–	–	–	–

NOTES: All major- and trace-element analyses were carried out at the Australian National University by X-ray fluorescence (XRF). All rare-earth element analyses were carried out at the University of Queensland by inductively coupled plasma mass spectrometry (ICP). The techniques are discussed in Morris (2000)

Reference

MORRIS, P. A., 2000, Composition of Geological Survey of Western Australia geochemical reference materials: Western Australia Geological Survey, Record 2000/11, 33p.

Appendix 3

Recorded gold production from JOHNSTON RANGE

Site	*Start date*	*End date*	*Ore treated (kt)*	*Contained metal (kg)*
Blue Peter	1937	1938	1.309	8.891
Bronzewing	1912	1912	0.045	1.867
Clamp's Central	1933	1950	9.534	0.197
Clamp's Central	1933	1950	9.534	242.522
Die Hardy	1933	1948	0.801	21.729
Effie's Reward	1911	1911	–	0.115
Evanston	1938	1960	61.493	1106.931
Evanston East	1938	1938	0.035	0.423
Evanston North	1938	1942	1.624	33.59
Everett	1938	1939	0.305	4.432
Goldies	1938	1938	0.203	1.342
Gravel Pit	1940	1943	–	2.466
Gravel Pit	1940	1943	0.243	4.984
Harbor Lights	1938	1938	0.342	2.5
Mt Jumbo	1936	1937	1.265	12.204
Mt King	1932	1933	0.133	3.669
Mt King Enterprise	1933	1939	0.507	6.286
Yarbu	1912	1912	0.01	0.511
Trier	1909	1909	0.002	0.189
Bullshead	1936	1936	0.104	0.49
Four B's	1939	1939	0.012	0.244
Gould R A	1979	1979	–	0.214
Lake Barlee	1937	1938	0.034	0.449

SOURCE: Townsend et al. (2000)

Reference

TOWNSEND, D. B., GAO MAI, and MORGAN, W. R., 2000, Mines and mineral deposits of Western Australia: digital extract from MINEDEX — an explanatory note: Western Australia Geological Survey, Record 2000/13, 28p.

The JOHNSTON RANGE 1:100 000 sheet covers the south-central portion of the BARLEE 1:250 000 sheet in the central part of the Southern Cross Province, which is in the central Archaean Yilgarn Craton. These Explanatory Notes describe the Precambrian rock types, and the structural and metamorphic geology of the granite–greenstone terrain. The greenstone stratigraphy and the constraints on the age of the various components of the greenstone succession, the deformation history, and its relationship to granitoid intrusion are discussed. Gold and base metal mineralization and the extensive Cainozoic regolith cover within the sheet area are also described.

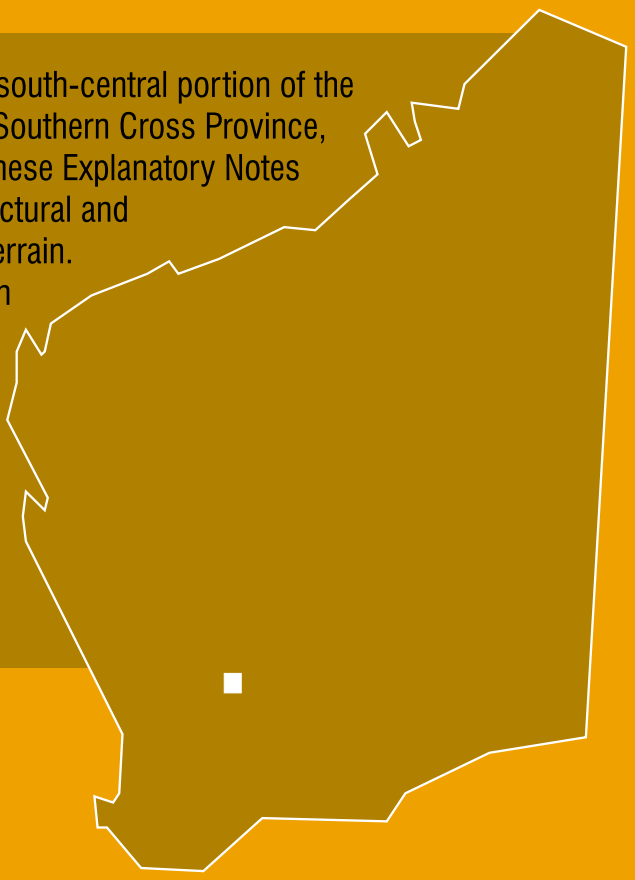

Further details of geological publications and maps produced by the Geological Survey of Western Australia can be obtained by contacting:

Information Centre
Department of Minerals and Energy
100 Plain Street
East Perth WA 6004
Phone: (08) 9222 3459 Fax: (08) 9222 3444
www.dme.wa.gov.au

AUSTRALIA 1 : 100 000 GEOLOGICAL SERIES

JOHNSTON RANGE

GEOLOGICAL SURVEY OF WESTERN AUSTRALIA

SHEET 2738

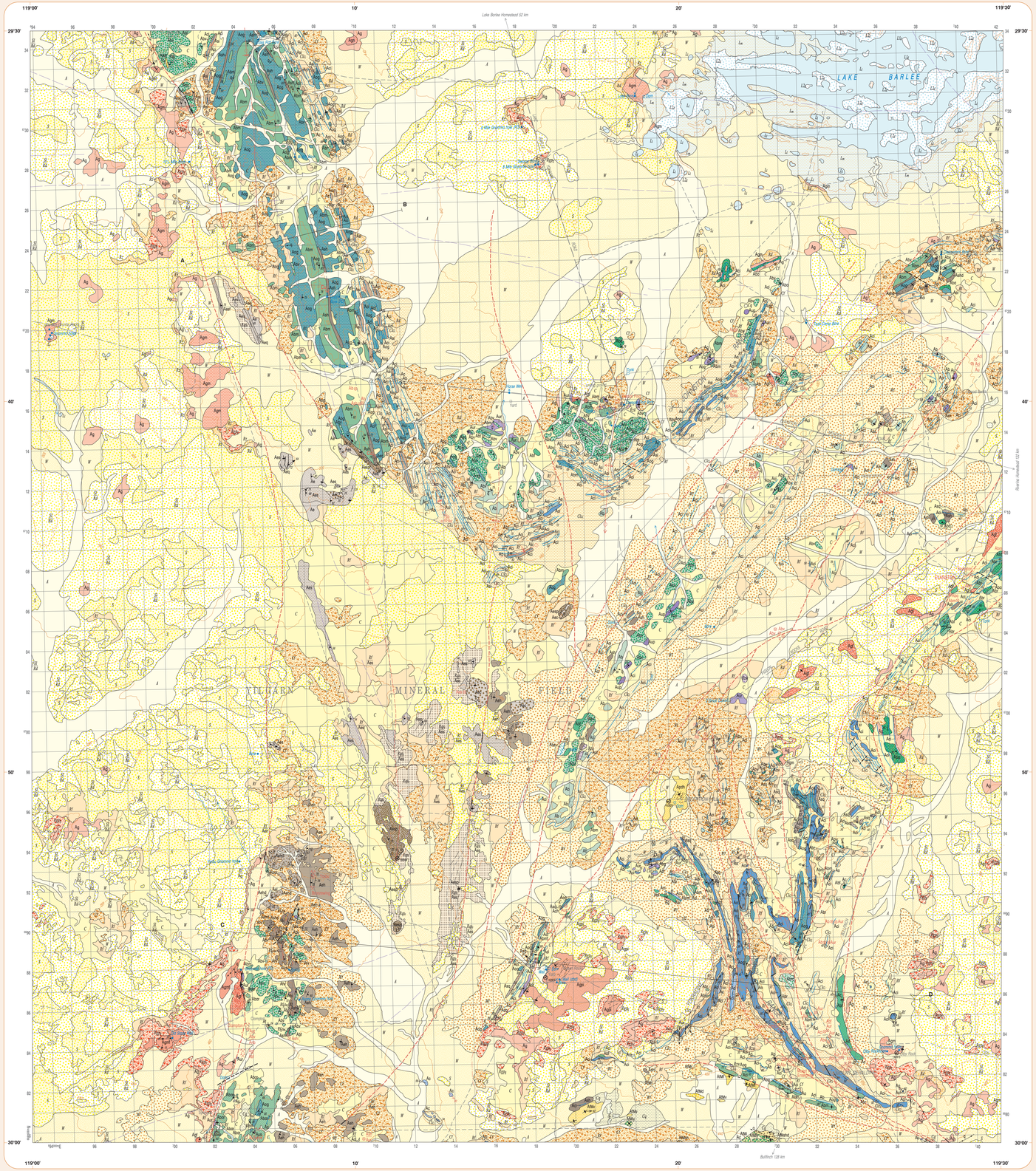

DIAGRAMMATIC SECTIONS

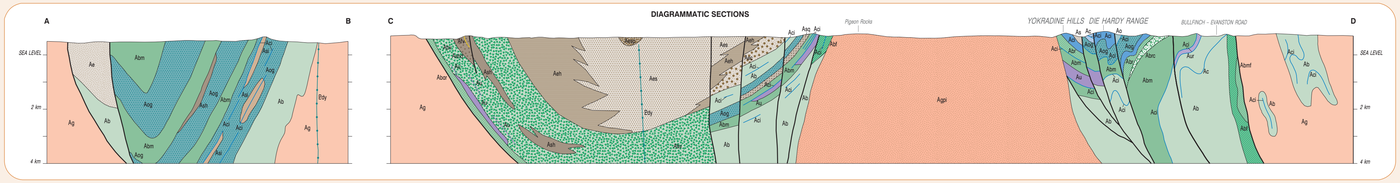

PHANEROZOIC

CAINOZOIC

Colluvial units
- *C* Mixed gravel from different rock types as proximal talus; includes sand and silt; locally ferruginous
- *Cf* Ferruginous gravel and reworked duricrust
- *Clo* Talus from banded iron-formation and chert; locally cemented
- *Cq* Quartz-vein debris

Sheetwash units
- *W* Clay, silt, and sand in extensive flats; locally ferruginous
- *Wf* Deposits with abundant ferruginous grit

Alluvial units
- *A* Clay, silt, sand, and gravel in channels and floodplains
- *Ap* Clay and silt in claypans

Lacustrine units
- *Ls* Saline playa lake deposits; mainly gypsiferous evaporite
- *Ld* Dune and lake deposits; active systems within and adjacent to playa lakes; unvegetated or poorly vegetated
- *Lm* Mixed dune, evaporite, and alluvial deposits adjacent to playa lakes

Lacustrine unit
- *Ld* Dune deposits; stabilized dunes within and adjacent to playa lakes; vegetated

Sandplain units
- *S* Residual and eolian sand
- *Sl* Yellow sand with minor pisolitic laterite, and silt and clay

Relict units
- *Rd* Siliceous and ferruginous duricrust, undivided
- *Rf* Lateritic duricrust; includes iron-cemented reworked products
- *Rlc* Lateritic duricrust; ironstone over ridge-forming units
- *Rgw* Gossanous units within strongly metasedimentary rock
- *Rggy* Quartzofeldspathic sand over granitoid rock; sparse granitoid outcrop
- *Rgs* Residual sandplain with scattered ironstu float
- *Rr* Silcrete; predominantly over granitoid rock
- *Rsx* Silica caprock over ultramafic rock

ARCHAEAN

Quartz veins and dykes
- *q* Quartz veins and dykes
- *g* Granitoid veins and dykes

c. 2730–2690 Ma
- *Ag* Granitoid rock, undivided; includes deeply weathered rock
- *Agf* Strongly foliated granitoid rock
- *Agm* Monzogranite
- *Agmf* Strongly foliated monzogranite
- *Agn* Gneissic granitoid
- *Agpi* **PIGEON ROCKS MONZOGRANITE:** biotite monzogranite, equigranular

c. 2729 Ma
- *Amb* Mafic gneiss (subsurface only)

<c. 2723 Ma
- *As* **DIEMALS FORMATION:** metasedimentary rock, undivided; includes deeply weathered rock
- *Asc* Polymictic conglomerate with minor sandstone; metamorphosed
- *Ash* Shale, mudstone, and siltstone; metamorphosed
- *Ashd* Andalusite-bearing pelite
- *Asl* Chlorite-bearing schist
- *Asq* Quartzite and metamorphosed quartz-rich sandstone
- *Ass* Metasandstone; dominantly quartz arenite; includes minor metamorphosed siltstone and quartz–mica schist
- *Assf* Foliated metasedimentary rock; includes quartz–mica schist
- *Assp* Metamorphosed pebbly sandstone

c. 2733 Ma
- *AMdd* Dacite; metamorphosed
- *AMdf* Strongly foliated felsic rock
- *AMdl* Andesite and basaltic andesite; metamorphosed
- *AMdy* Andesite with quartz–ederite–filled cross-bedding; metamorphosed
- *AMdv* Volcaniclastic shale and siltstone; metamorphosed; locally ferruginous
- *AMdvd* Foliated metapelite with andalusite(–staurolite)
- *AMr* Rhyolite; metamorphosed
- *AMv* Fine-grained felsic volcanic rock; metamorphosed

MARDA COMPLEX
- *As* Metasedimentary rock, undivided; typically deeply weathered
- *Ash* Shale and siltstone; metamorphosed
- *Ashd* Foliated pelitic rocks with andalusite or staurolite; locally with cordierite
- *Asi* Metasedimentary rock; includes shale, siltstone, chert, and banded iron-formation; deeply weathered and ferruginized
- *Asq* Quartz-rich metasedimentary rock; includes quartzite and recrystallized chert
- *Ass* Metasandstone
- *Ac* Banded chert and ferruginous banded chert; metamorphosed
- *Aci* Banded iron-formation and ferruginous banded chert; bocil jaspilite; metamorphosed

- *Af* Fine-grained felsic rock, undivided; typically deeply weathered; metamorphosed
- *Afv* Fine-grained felsic volcanic rock; metamorphosed

c. 3023 Ma
- *Apdh* **DECEPTION HILL PORPHYRY:** massive quartz–feldspar porphyry; metamorphosed

- *Ao* Metamorphosed, medium- to coarse-grained mafic rock; typically deeply weathered
- *Aog* Metagabbro; medium- to coarse-grained; includes local quartz gabbro

- *Ab* Metamorphosed mafic rock; mainly fine-grained; typically deeply weathered
- *Aba* Amphibolite; fine- to medium-grained; commonly foliated
- *Abar* Amphibolite retrogressed to greenschist facies assemblages
- *Abe* Epidotized metabasalt
- *Abf* Strongly foliated, metamorphosed mafic rock; local amphibolite
- *Abi* Basaltic andesite; metamorphosed
- *Abm* High-Mg basalt with relict pyroxene spinifex and/or variolitic textures; metamorphosed
- *Abmf* Strongly foliated high-Mg basalt; locally variolitic; metamorphosed
- *Abr* Strongly foliated tremolite- and chlorite-rich rock; probably after high-Mg basalt
- *Abrc* Strongly foliated tremolite- and chlorite-rich rock; probably after high-Mg basalt; strongly carbonated
- *Abt* Mafic tuff; metamorphosed
- *Abv* Metabasalt; massive to weakly foliated
- *Abx* Mafic breccia; metamorphosed

- *Au* Metamorphosed ultramafic rock; typically deeply weathered
- *Aup* Metamorphosed peridotite; typically serpentinized
- *Aur* Tremolite–chlorite(–talc) schist
- *Aus* Serpentinite
- *Aut* Talc–tremolite(–chlorite) schist

YILGARN CRATON

INTERPRETED BEDROCK GEOLOGY

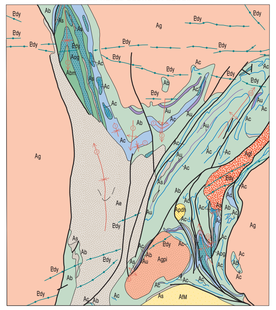

- Mafic dyke
- Ag Agf Agm — Granitoid rock
- Agpi Pigeon Rocks Monzogranite
- Ae Diemals Formation
- AMd Marda Complex
- As Ac — Metasedimentary rock; Metamorphosed banded iron-formation, chert, and shale with associated mafic rock
- Apdh Deception Hill Porphyry
- Aog Metagabbro
- Ab Abm — Ab Metabasalt dominant; Abm Metamorphosed high-Mg basalt
- Au Metamorphosed ultramafic rock

SCALE 1:100 000

0 5 10 15 20 Kilometres

Geology by S. Wyche, S. F. Chan, J. E. Greenfield, and A. Riganti 1997–1998

Geochronology by D. R. Nelson

Edited by N. Tetlow, G. Luon, and C. Brien

Cartography by G. Fletcher, B. Williams, and K. Greenberg

Topography from the Department of Land Administration Sheet SH 50-8, 2738, with modifications from geological field survey

Published by the Geological Survey of Western Australia. Copies available from the Information Centre, Department of Minerals and Energy, 100 Plain Street, East Perth, WA, 6004. Phone (08) 9222 3459. Fax (08) 9222 3444

This map is also available in digital form

Printed by the Bonds Print Group, Western Australia

The recommended reference for this map is:
WYCHE, S., CHEN, S. F., GREENFIELD, J. E., and RIGANTI, A., 2000, Johnston Range, W.A. Sheet 2738: Western Australia Geological Survey, 1:100 000 Geological Series

Geological boundary
- exposed
- concealed, interpreted from aeromagnetic data

Structural symbols are labelled according to the sequence of deformation events, where known.
- Yilgarn
- D_1
- D_2 and D_3
- D_4
- D_5

Fault or shear
- exposed
- concealed
- concealed, interpreted from aeromagnetic data
- horizontal relative displacement

Strongly foliated rock

Fold, showing axial trace and generalized plunge direction
- anticline, exposed
- synclime, exposed, concealed
- antiform, exposed

Small-scale fold axis, showing trend and plunge
- unspecified
- Z-vergence
- M-vergence

Bedding, showing strike and dip
- inclined
- vertical
- overturned
- trend of bedding

Way-up indicator
- sedimentary structure
- graded bedding

Foliation, showing strike and dip
- inclined
- vertical

Cleavage, showing strike and dip
- inclined
- vertical

Stretching lineation, showing trend and plunge

Axis of cremulation, showing trend and plunge

Bedding–cleavage intersection lineation, showing trend and plunge

Airphoto lineament
- unspecified
- fracture pattern

Aeromagnetic lineament

Isotopic age determination site with identification number — 14305

Formed road

Major track

Track

Fence, generally with track

Homestead — Diemals

Locality — Crampton

Building

Yard — Yard

Horizontal control; major, minor

Breakaway

Sand dune

Contour line, 20 metre interval — 400

Watercourse

Gnamma hole — Gnamma hole

Rockhole — Rockhole

Soak, spring — Soak, Spring

Bore, well — Bore, Well

Windpump

Dam, tank — Dam, Tank

Abandoned — (dam)

Position doubtful — (PD)

Mining centre — EVANSTON

Mine (gold, unless otherwise indicated) — Mount Jumbo

Mine, abandoned (for commodities other than gold)

Opencut

Quarry or pit

Prospect

Treatment plant

Subsurface data from drillhole, costean, or shallow shaft — Abv

Mineral occurrence
- Copper — Cu

SHEET INDEX

1:100 000 maps shown in black

1:250 000 maps shown in brown

DEPARTMENT OF MINERALS AND ENERGY
L. C. RAWCHD, DIRECTOR GENERAL

GOVERNMENT OF WESTERN AUSTRALIA
HON. NORMAN MOORE, M.L.C.
MINISTER FOR MINES

GEOLOGICAL SURVEY OF WESTERN AUSTRALIA
DAVID BLIGHT, DIRECTOR

SCALE 1:100 000

1000 0 1 2 3 4 5 6 7 8 9 10 Metres Kilometres

UNIVERSAL TRANSVERSE MERCATOR PROJECTION
HORIZONTAL DATUM: GEOCENTRIC DATUM OF AUSTRALIA 1994
VERTICAL DATUM: AUSTRALIAN HEIGHT DATUM

Grid lines indicate 1000 metre interval of the Map Grid Australia Zone 50

GDA

The Map Grid Australia (MGA) is based on the Geocentric Datum of Australia 1994 (GDA94)
GDA94 positions are compatible within one metre of the datum WGS84 positions

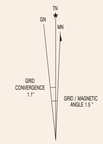

True north, grid north and magnetic north are shown diagrammatically for the centre of the map. Magnetic north is current for 2000 and moves westerly by about 0.1° in 3 years.

JOHNSTON RANGE

SHEET 2738 FIRST EDITION 2000

Version 1.1 — August 2003